NASA Technical Memorandum 102560

Demonstration of Capabilities of High Temperature Composites Analyzer Code HITCAN

Surendra N. Singhal and Joseph J. Lackney
Sverdrup Technology, Inc.
NASA Lewis Research Center Group
Cleveland, Ohio

Christos C. Chamis and Pappu L.N. Murthy
National Aeronautics and Space Administration
Lewis Research Center
Cleveland, Ohio

March 1990

(NASA-TM-102560) DEMONSTRATION OF CAPABILITIES OF HIGH TEMPERATURE COMPOSITES ANALYZER CODE HITCAN (NASA) 56 p CSCL 20K

N90-19629

Unclas
G3/39 0272820

NASA

TABLE OF CONTENTS

DEMONSTRATION OF CAPABILITIES OF HIGH TEMPERATURE COMPOSITES ANALYZER CODE HITCAN

Surendra N. Singhal and Joseph J. Lackney
Sverdrup Technology, Inc.
NASA Lewis Research Center Group
Cleveland, Ohio 44135

Christos C. Chamis and Pappu L.N. Murthy
National Aeronautics and Space Administration
Lewis Research Center
Cleveland, Ohio 44135

ABSTRACT

The present report demonstrates the capabilities of a high temperature composites analyzer code, HITCAN which predicts global structural and local stress-strain response of multilayered metal matrix composite structures. The response can be determined both at the constituent (fiber, matrix, and interphase) and the structure level and including the fabrication process effects. The thermo-mechanical properties of the constituents are considered to be nonlinearly dependent on several parameters including temperature, stress, and stress rate. The computational procedure employs an incremental iterative nonlinear approach utilizing a multifactor-interactive constituent material behavior model. Various features of the code are demonstrated through example problems for typical structures.

INTRODUCTION

Background Information

There is an increasing effort on pushing the performance limit of structural composite materials for developing 21st century propulsion systems. In this regard, the potential of high temperature metal matrix composite (HTMMC) materials has already been recognized. The thermo-mechanical properties of components made from HTMMC materials exhibit a nonlinear dependence on parameters such as temperature, stress, and stress rate. This phenomenon may alter the structural response significantly. Experimental investigations being high in cost, computational models including nonlinear material behavior simulating the real-life response of components made from HTMMC materials are required.

The need for developing multilevel analysis models for multilayered fibrous composites was recognized almost 2 decades ago (Ref. 1) and a multilevel analysis computer code was developed subsequently (Ref. 2). Research related to various aspects of HTMMC materials and structures has been conducted at the Lewis Research Center of the National Aeronautics and Space Administration (NASA) for several years. Building upon parts of this research effort, a high temperature composites analyzer code HITCAN, has been developed.

HITCAN-Brief Description

HITCAN is a general purpose code for predicting global structural and local stress-strain response of arbitrarily oriented, multilayered high temperature metal matrix composite structures both at the constituent (fiber, matrix, and interphase) and the structure level. The thermo-mechanical properties of constituents are considered to be nonlinearly dependent on several parameters including temperature, stress, and stress rate. The computational procedure employs an incremental iterative nonlinear approach based on a multifactor-interactive constituent material behavior model of product series form (Ref. 3).

HITCAN presents a synergistic combination of NASA developed codes, MHOST and METCAN. MHOST (Ref. 4) and METCAN (Ref. 5 to 9) are finite element structural analysis, and multilevel nonlinear material behavior codes, respectively. HITCAN offers a self-contained (independent of commercial codes) modular code including standard functions of the finite element analysis and complex nonlinear models of composite micro- and macro-mechanics theories. HITCAN will help in material selection for specific applications, in analyzing sensitivity of structural response to various system parameters, and in providing structural response at all levels of material constituents.

User-friendliness was kept in mind during the development of HITCAN code. For instance, it includes a material property database for commonly used aerospace fiber and matrix materials. The user needs to specify only a code name of the material (rather than having to input all the properties) in the HITCAN input. HITCAN automatically searches, selects, and updates the appropriate properties from its database. A list of materials and their properties for the materials coded in the HITCAN database can be found in Ref. 7. The database includes graphite, boron, silicon carbide, and tungsten fibers, and aluminum, titanium, copper, magnesium, and beryllium matrix materials.

HITCAN is a research tool created by combining several products of the high temperature research conducted at NASA. It is continually enhanced as more research bears fruit. It has, however, already been developed and tested for many features qualifying it as a useful design tool.

The source code, HITCAN consists of about 10,000 FORTRAN statements. The accompanying codes METCAN and MHOST comprise of about 7,000 and 50,000 statements, respectively. A complete documentation of HITCAN including theoretical developments, user's manual, and demonstration manual are expected to be available in near future.

Objective of Present Report

The objective of the present report is to summarize HITCAN's capabilities and application versatility. Various features of the code are demonstrated through illustrative examples for typical structures including beam, plate, ring, curved panel, and a built-up structure.

FEATURES

HITCAN is capable of predicting global structural and local stress-strain response of multilayered high temperature metal matrix composite structures. It can perform modal and buckling analyses. Each layer of the composite can be of different material and can be arbitrarily oriented. The current version of the code can handle any number of layers. HITCAN is designed for metal matrix composites only. NASA has developed separate codes for analyzing structures made of other types of materials (Ref. 10 to 12).

The current version of the code is based only on rectilinear coordinates. Nevertheless, arbitrary shaped geometries can be modeled using interpolators included in the mesh generation segment of the code.

In general, the analysis capabilities of HITCAN are primarily governed by those of its' ingredient codes, MHOST (Ref. 4) and METCAN (Ref. 7).

MHOST is capable of handling standard two- and three-dimensional, beam, and shell structural elements, all types of boundary conditions, most types of loadings (concentrated, distributed, pressure, temperature, static, transient, cyclic, and impact), anisotropic composite materials, elastic and inelastic analyses, eigenvalue extraction for buckling and modal analyses, and various types of structures (such as beam, plate, ring, curved panel, and built-up structures).

METCAN is capable of modeling thermo-mechanical properties as multifactor - interactive functions of temperature, stress, stress rate, and additional factors such as cyclic loading. METCAN treats material nonlinearity at the constituent level. The composite properties are synthesized from constituent instantaneous properties through composite micro- and macro-mechanics models. METCAN includes the dependence of the behavior of metal matrix composites on fabrication process variables, in-situ fiber and matrix properties, bonding between the fiber and matrix, and properties of an interphase between the fiber and matrix.

The current version of HITCAN includes most (but not all) features of MHOST and METCAN. Work is continuing on including more features into HITCAN. Table I lists HITCAN features. The features that are demonstrated through example problems in the present report, are marked 'tested' in italic letters in Table I. Although the enhancement of the code continues, in its current form, it is applicable to a wide variety of composite structural analysis problems.

COMPUTATIONAL PROCEDURE

Structures made of composites consist of four levels of distinct material identity, namely structural component, laminate, ply, and fiber/matrix/interphase constituents, marked in bold italic letters in Figure 1. The component is fabricated by putting several types of laminates together. Each laminate is made from several plies stacked in different directions. Each ply, in turn, is made from basic constituent materials, i.e., fiber, matrix, and interphase. The interphase represents the material formed between the fiber and matrix. Material properties are generally available at the basic most, i.e. the constituent level. Material properties at the ply level are obtained using micromechanics equations based on the unit cell square array approach. In this approach, the ply level is represented by a unit cell as shown in Figure 2. In a typical ply, these cells are assumed to have been arranged in a square array. Within each unit cell, there are 3 regions of material non-unifirmity as shown in Figure 2.

The structural response is calculated by using the finite element approach. In this approach, the structure is divided into several finite size elements. Each element can be treated as a specific type of laminate. The finite element approach thus requires that the material properties be made available at the laminate level. Also, the stress-strain response predicted by the finite element approach is at the laminate level. But, the constituent material properties, required to be input for the finite element analysis at the laminate level, tend to depend on the constituent level stress response. There is thus a need for iterative computations at several different levels of composite materials.

Figure 1 shows the approach used by HITCAN for analyzing composite structures. The left part of Figure 1 depicts the determination of laminate properties based on known constituent properties. The top part depicts the finite element analysis which provides the structural response at the laminate level. And, the right part shows the determination of the structural response at the constituent level. Finally, the bottom left part shows the updating of constituent material properties based on input parameters and calculated constituent stress response.

HITCAN accomplishes the approach shown in Figure 1 by calling upon the finite element code, MHOST (Ref. 4), and the multilevel material behavior code, METCAN (Ref. 7). HITCAN manages the flow of information between MHOST and METCAN. It also serves the function of transforming the input/output between MHOST and METCAN to the desired form. In addition, HITCAN contains FORTRAN coding for generating the finite element model of the structure.

The flow-chart in Figure 3 shows major computational procedural steps, in the order in which they are executed by the code.

Step 1. Finite Element Model Generation

HITCAN generates a finite element model of the structure, based on coordinates of a few representative points. This is accomplished by interpolators coded in HITCAN. The temperature and pressure loadings are also input only at the representative points, to be interpolated for the rest of the model automatically by the code.

Notice that the finite elements are at the laminate level but the material properties input in step 1 are at the constituent level.

Step 2. Constituent Material Property Generation

Based on reference constituent material properties available at the end of Step 1, METCAN generates constituent material properties including an interactive dependence on parameters such as temperature, stress, and stress rate before the next load step (see multifactor interactive equations in Ref. 3, 5, and 9). This step is illustrated through the item, A, marked in boxed letter in Figure 1.

Step 3. Laminate Material Property Generation

The material properties available at the end of Step 2 need to be converted to those at the laminate level before conducting the finite element analysis. METCAN accomplishes Step 3 by using micro- and macro-mechanics theories. This step is illustrated through items, B and C, marked in boxed letters in Figure 1.

Step 4. Global Structural Response

All information necessary for the global finite element structural analysis becomes available at the end of Step 3. MHOST accomplishes Step 4 by calculating the structural response at the laminate level. This step is illustrated by the item, D, marked in boxed letter in Figure 1.

Step 5. Constituent Structural Response

Based on laminate structural response calculated in Step 4, METCAN calculates the ply and constituent level structural response using macro- and micro-mechanics theories, shown by items, E and F, marked in boxed letters in Figure 1.

Step 6. Updating of Constituent Material Properties

Since the constituent material properties depend on calculated constituent stress response which, in turn, depends on constituent material properties, an iterative scheme is used to obtain both the structural response and material properties which are compatible with each other. For a specific load step, the ply level response (strains) and structure level response (strains at nodes) are compared at the end of each iteration with the response at the end of the previous iteration. Notice that the ply level response is in the local materials coordinate system whereas the structure level response is in the global structural coordinate system. Figure 1 shows both of these coordinate systems. If the difference in the response for two consecutive iterations is within a predetermined tolerance level, it is assumed that the solution has reached a satisfactory level of convergence. This step is illustrated through a diamond-shaped block in Figure 3.

Additional Features

Additional features such as fiber degradation and fabrication-induced stresses have been incorporated in the computational procedure. Fiber degradation is accounted for by decreasing the diameter of the fiber based on a user specified fraction of the original fiber diameter (refer to Figure 4). This creates an interphase, of a specified thickness, between the fiber and matrix. The stresses during fabrication are calculated by defining the cool down process from the consolidation temperature to reference temperature as a specified load history added prior to the application of actual loads.

THEORETICAL BASIS

The theoretical basis follows the steps described in the previous section titled, 'Computational Procedure' Figure 3 also outlines these steps.

1. Finite Element Model Generation

The nodal values of geometrical coordinates, and temperature and pressure loadings are interpolated using linear and/or cubic splines depending on the number of points input. The coding for the finite element model generation was adopted from Ref. 13 to 15.

2. Constituent Material Property Generation

A modular interactive Chamis-Hopkins model (Ref. 3, 5, and 9) accounting for the effect on constituent material properties of several parameters such as temperature, stress, and stress rate is employed. For reader's convenience, the model is reproduced below.

(1) Mechanical property (moduli, strength) P_M

$$\frac{P_M}{P_{Mo}} = \left[\frac{T_M - T}{T_M - T_o}\right]^n \left[\frac{S_F - \sigma}{S_F - \sigma_o}\right]^m \left[\frac{\dot{S}_F - \dot{\sigma}_o}{\dot{S}_F - \dot{\sigma}}\right]^l$$

(2) Thermal property (expansion coefficients, thermal conductivity, heat capacity) P_T

$$\frac{P_T}{P_{To}} = \left[\frac{T_M - T_o}{T_M - T}\right]^n \left[\frac{S_F - \sigma_o}{S_F - \sigma}\right]^m \left[\frac{\dot{S}_F - \dot{\sigma}}{\dot{S}_F - \dot{\sigma}_o}\right]^l$$

where

P_M	denotes the current mechanical property of interest
P_T	denotes the current thermal property of interest
P_{Mo} , P_{To}	are corresponding properties at reference conditions
T_M	is the melting temperature
T	is the current temperature
T_o	is the reference temperature at which P_{Mo} & P_{To} are determined
S_F	is the fracture stress determined at T_o conditions
σ	is the current stress
σ_o	is the reference stress at which P_{Mo} & P_{To} are determined
$\dot{S}_F$	is an appropriately selected stress rate, for example, the stress rate at which penetration occurs during impact
$\dot{\sigma}_o$	is the stress rate at which P_{Mo} & P_{To} are determined
$\dot{\sigma}$	is the stress rate, and
n,m,l	are empirical constants

3. **Laminate Material Property Generation**

Due to easy availability in numerous publications of micro- and macro-mechanics theories used for the laminate material property generation, they are not reproduced in the limited space of the present report. They can be found in Ref. 16.

4. **Global Structural Response**

The finite element theory is well published and thus not reproduced here. The relevant mathematical equations can be found in Ref. 16.

5. **Constituent Structural Response**

These relationships, available widely, are not reproduced in the present report. They can be found in Ref. 5.

6. **Updating of Constituent Material Properties**

These relationships have already been cited in item 2 above.

Additional Features:

Fiber degradation, based on the reduction in fiber diameter, is governed by the equation given below (refer to Figure 4).

$$D = (1-F)D_o$$

Where

D is the reduced fiber diameter,

F is the fiber degradation parameter (= fraction of original fiber diameter), and

D_o is the original fiber diameter

Thermal residual stresses due to the fabrication process are calculated by adding a cool down load history from the consolidation temperature to reference temperature before applying the actual load history.

DEMONSTRATION PROBLEMS

HITCAN capabilities are demonstrated through illustrative examples for five types of structures. Four of these represent basic geometries that are the building blocks of most structures of practical interest. They are beam, plate, ring, and curved panel. The fifth one is a built-up structure. Figures 5 to 9 show the geometrical shape along with necessary dimensions. The finite element mesh sizes used are (12,4), (6,4), (9,4), (8,8), and (4,8) for beam, plate, ring, curved panel, and built-up structure, respectively. The first number in the mesh size represents number of elements along the longer side and the second number along the smaller side.

For the ease of comparison and for consistency, the laminate material was kept the same for all the example structures. The material chosen is Si C/Ti-15-3-3-3 (where Si C stands for Silicon Carbide fiber and Ti-15-3-3-3 for an alloy of titanium with 15% Vanadium, 3% Aluminum, 3% Chromium, and 3% Tin). This material was chosen because it has already received wide recognition as a viable candidate for some of the high temperature applications associated with the National Aerospace Plane (NASP). The material properties of Si C fiber and Ti-15-3-3-3 matrix, in the unstressed reference state, are given in Table II. In all cases, the reference temperature was 70 °F both for material properties and thermal loading, the fiber volume ratio was 0.4, the laminate consisted of four ply layers (except for the built-up structure with a 4-layered top surface, 2-layered bottom surface, and 4-layered spars), the finite element was a four-node isoparametric shell element with six degrees of freedom per node, and the exponents used for the multifactor-interactive constitutive material behavior model (defined in 'Constitutive Material Property Generation' of the 'Theoretical Basis' section) are given in Table III. The ply orientations were chosen to be (0/± 45/90) for all structures, except for built-up structure with a $(90/0)_s$ top surface, $(90)_s$ bottom surface, and 4(0) spars. The first ply is at the top surface and the last ply is at the bottom surface. The ply orientation of 0 deg. means fibers oriented in the x-direction. Other, i.e. nonzero, orientations represent fibers oriented at the specified angle of rotation with respect to x-axis towards the y-axis. The laminate of Figure 1 shows ply orientations used for beam, plate, ring, and curved panel.

Several types of analyses, marked 'tested' in italics in Table I, were conducted for each type of structure. The analyses tested include static, buckling, modal, and load stepping. All analyses were based on multilevel-interactive material behavior. The sensitivity of structural response to various parameters was determined by repeating the load stepping analysis for various forms of multifactor-interactive constitutive models, for various ply orientations, and for various additional features including fiber degradation and fabrication-induced stresses.

Static Analysis

The static analysis was conducted for a combined thermal and mechanical load applied in one step, not including any additional features such as fiber degradation and fabrication-induced stresses. The loadings and boundary conditions used are same as shown in Figures 5 to 9 for beam, plate, ring, curved panel, and built-up structure, respectively, except that the load was applied in one step for the static analysis. The material properties, given in Table II, remained constant at the reference value. A summary of input parameters used for the static analysis is given in Table IV.

Buckling Analysis

The buckling analysis was first conducted for mechanical loading only. The first buckling mode was calculated in each case (the code is capable of calculating as many modes as desired). The analysis was then repeated for two cases; for mechanical loading including fiber degradation and for combined thermo-mechanical loading without fiber degradation. For the first case, the fiber was degraded by a factor of one-tenth of its original diameter. The loadings and boundary conditions used are shown in Figures 10 to 14 for all five structures. A summary of input parameters used for the buckling analysis is given in Table V.

Modal Analysis

The modal analysis was performed for a combined thermal and mechanical load applied in three steps of increasing load, not including the additional features; fiber degradation and fabrication-induced stresses. Four modes were calculated (the code is capable of calculating as many modes as desired). The loadings and boundary conditions used are shown in Figures 5 to 9 for beam, plate, ring, curved panel, and built-up structure, respectively. Material properties vary nonlinearly as the load increases, from the reference values listed in Table II. A summary of the input parameters used for the modal analysis is given in Table VI.

Load Stepping Analysis

The load stepping analysis is essentially a piecewise linear analysis where the load is applied incrementally in several steps with material properties updated at the end of each load step.

The load stepping analysis was first performed for the base case using loadings, boundary conditions, material properties, ply orientations, and the most general form of the constitutive model used for the 'Modal Analysis' described above. The base case did not include any additional features. The load stepping analysis was then repeated by varying one parameter or by invoking one feature at a time, for the derivative cases listed below.

Constitutive Models: Four cases of constitutive models, different from the most general model used for the base case, were used. They are: the constant material property case, material properties dependent on temperature only, material properties dependent on stress only, and material properties dependent on stress rate only.

Ply Orientations: Two cases of ply orientations, different from the base case's unsymmetric orientations, were used. They are: the symmetric orientation of $(0/45)_s$, and balanced orientation of $(0/90)_s$.

Fiber Degradation: Fiber degradation was included. An interphase was created between the fiber and matrix. The thickness of the interphase was chosen to be equal to one-tenth of the original fiber diameter. The final diameter of the fiber was thus reduced to nine-tenths of its original diameter. For the demonstration problems discussed in the present report, the properties of the interphase were taken as an average of the fiber and matrix properties.

Fabrication-Induced Stresses: A sequence of fabrication thermal loading, shown in Figure 15, was included before applying combined thermal and mechanical loadings of Figures 5 to 9. Note that a consolidation temperature of 1000 °F was used for the problems demonstrated in the present report. The real consolidation temperature could be different.

RESULTS

The results for various types of analyses, described in the 'Demonstration Problems' section are pooled together for presentation in the form of Figures and Tables. Only representative results are included in the present report. HITCAN outputs with a complete set of results have been archived in NASA's VM computer system. The results for static analysis, being similar to the constant material property case of the load stepping analysis, are not included in the present report. The buckling analysis results are presented in Figures 10 to 14. The critical buckling load with and without fiber degradation is computed from eigenvalues output by HITCAN. The natural vibration frequencies are presented along with stress and displacement results for the base case load stepping analysis.

Figures 16 to 20 show base case results including natural frequencies, displacements, and constituent and ply level stresses. The displacements are in the global structural coordinate system and the stresses in the local materials coordinate system. Both of these coordinate systems are shown in Figure 1. Letters A, B, and C, used in Figures 16 to 20 are for various regions of constituent material nonuniformity, defined in Figure 2. The displacement and ply stress results of the sensitivity analysis with respect to various forms of constitutive models, various ply orientations and fiber degradation and fabrication-induced stresses are tabulated in Figures 21 to 25. For the sake of brevity, the response is compared with the base case at the end of the third load step only. The effect of stress rate was found negligible in all cases, due to the very nature of the problems chosen. This effect will show up in the transient analysis.

The effect of using different forms of constitutive models was analyzed further, as shown in Figures 26 to 30. These Figures show the importance of using material behavior models which are dependent on applied temperature and calculated stress response. Notice that the vertical axis of Figures 26 to 30 shows percentage increase in the total displacement due to a change in the form of the constitutive model, i.e. these Figures depict increase in total displacement caused by the degradation of material properties according to the Chamis-Hopkins model. The increase in total displacement is measured from the case when material properties are considered constant. The total displacement here refers to the displacement caused both by thermal and mechanical loadings. In Figures 26 to 30, the label 'Temperature Effect' refers to percentage increase in total displacement when the material properties are made temperature dependent only. Similarly, the label 'Stress Effect' refers to percentage increase in total displacement when the material properties are made stress dependent only. And, the label 'Combined Effect' refers to percentage increase in total displacement when the material properties are made dependent on temperature and stress simultaneously.

A simple derivation for the effect of nonlinear material property variations on beam deflection is presented in the Appendix. The Appendix shows separate, combined (i.e., superposed), and coupling effects of temperature, stress, and stress rate on beam deflection. Notice that the effect on the structural response of such material behavior models will increase with increasing thermal and mechanical loads, typical of aerospace applications.

Since, the purpose of the present report is to demonstrate the capabilities of HITCAN rather than to provide results, a detailed discussion of the results is not included. Also, due to the unavailability of results in open literature for the complex problems modeled by HITCAN, it has not been possible to provide comparisons. However, the code has been verified for some classical simplified linear cases (Ref. 17).

CONCLUSIONS

The capabilities of a high temperature composites analyzer code, HITCAN, have been demonstrated. HITCAN was developed for performing most of the typical structural analysis tasks for designing with multilayered metal matrix composites. The code is modular, open-ended, and user-friendly. It employs multifactor-interactive constitutive material behavior models. It includes additional features such as fiber degradation and fabrication-induced stresses. Because of the multilevel analysis approach, HITCAN has the utility for studying the influence of individual constituent in-situ behavior on global structural response. Several features of HITCAN have been demonstrated through example problems. These features make HITCAN a powerful, cost-effective tool for analyzing/designing metal matrix composite structures and components.

REFERENCES

1. Chamis, C.C., "Design Oriented Analysis and Synthesis of Multilayered-Filamentary Structural Panels," Ph.D. thesis, Case Western Reserve University, Cleveland, Ohio, 1967.

2. Chamis, C.C., "Computer Code for the Analysis of Multilayered Fiber Composites-User's Manual," NASA TN-D-7013, 1971.

3. Chamis, C.C. and Hopkins, D.A., "Thermoviscoplastic Nonlinear Constitutive

Relationships for Structural Analysis of High Temperature Metal Matrix Composites," NASA TM-87291, 1985.

4. Nakazawa, S., "The MHOST Finite Element Program: 3-D Inelastic Analysis Methods for Hot Section Components. Volume II - User's Manual," NASA CR-182235, 1989.

5. Hopkins, D.A., "Nonlinear Analysis for High-Temperature Multilayered Fiber Composite Structures," NASA TM-83754, 1984.

6. Hopkins, D.A. and Chamis, C.C., "A Unique Set of Mircromechanics Equations for High Temperature Metal Matrix Composites," NASA TM-87154, 1985.

7. Murthy, P.L.N. and Hopkins, D.A., "Metal Matrix Composites Analyzer: METCAN User's Guide," NASA Report (in Draft Form), 1988.

8. Chamis, C.C., Murthy, P.L.N., and Hopkins, D.A., "Computational Simulation of High Temperature Matrix Composites Cyclic Behavior," NASA TM-102115, 1988.

9. Murthy, P.L.N., Hopkins, D.A., and Chamis, C.C., "Metal Matrix Composite Micromechanics: In-Situ Behavior Influence on Composite Properties," NASA TM-102302, 1989.

10. Murthy, P.L.N. and Chamis, C.C., "Integrated Composites Analyzer (ICAN): User's and Programmer's Manual," NASA TP-2515, 1986.

11. Murthy, P.L.N. and Chamis, C.C., "ICAN: Integrated Composites Analyzer," Journal of Composites Technology & Research, Volume 8, No. 1, Spring, 1986, pp. 8-17.

12. Chamis, C.C., Aiello, R.A., and Murthy, P.L.N., "Fiber Composites Sandwich Thermostructural Behavior: Computational Simulation," NASA TM-88787, 1986.

13. Aiello, R.A., "Composite Blade Structural Analyzer (COBSTRAN) User's Manual," NASA TM-101461, 1989.

14. Aiello, R.A., "Composite Blade Structural Analyzer (COBSTRAN) Demonstration Manual," NASA TM-101957, 1989.

15. Aiello, R.A. and Chamis, C.C., "Composite Blade Structural Analyzer (COBSTRAN) Theoretical/Programmer's Manual," NASA TM-101958, 1989.

16. Nakazawa, S., "3-D Inelastic Analysis Methods for Hot Section Components," NASA Contractor Report 179494, 1987.

17. Aiello, R.A. and Chi, S., "Advanced Composite Turboprop: Modeling, Structural and Dynamic Analyses," ASME Paper 87-GT-78, presented at the Gas Turbine Conference and Exhibition, Anaheim, California, May 31 - June 4, 1987.

Appendix

Subject: A simple derivation for the effect of nonlinear variations of material properties on beam deflection.

Problem: Consider a cantilever beam with concentrated end load (see Figure 5). Consider the effect of variable modulus of elasticity only.

Objectives: (1) To demonstrate the change in beam deflection due to the change in the modulus of elasticity as affected by temperature, stress, and stress rate, separately.

(2) To demonstrate the change in beam deflection due to the change in the modulus of elasticity as affected by temperature, stress, and stress rate, simultaneously.

(3) To demonstrate the difference between (1) and (2), i.e. the coupling effect of variables affecting the modulus of elasticity.

Notation: **Modulus of elasticity**

$E = (E_o).(E_T).(E_\sigma).(E_{\dot{\sigma}})$ (NOTE: This is an abbreviated form of equation (1) in 'Constituent Material Property Generation' step in the 'Theoretical Basis' section.)

where E_o is the value of E for the constant property case
E_T is temperature dependent component of E
E_σ is stress dependent component of E
$E_{\dot{\sigma}}$ is stress rate dependent component of E

Beam deflection at the end

Let, $w = A/E$ (NOTE: This simple formula doesn't quite apply to the problem we ran on HITCAN. It applies only under certain assumptions. Nevertheless, it serves the purpose of carring out the objective of this Appendix in a simple, yet reasonable manner).

Where w_o is the value of w for the constant property case
w_T is temperature component of w
w_σ is stress dependent component of w
$w_{\dot{\sigma}}$ is stress rate dependent component of w

and Δw_T is increase in w due to temperature dependence only
Δw_σ is increase in w due to stress dependence only
$\Delta w_{\dot{\sigma}}$ is increase in w due to stress rate dependence only
Δw_C is cumulative increase in w due to all components added together
Δw is increase in w due to simultaneous effect of all components

Derivations: (i) Deflection due to one component at a time

$w_o = A/E_o$ for the constant property case

$w_T = (A/E_o).(1/E_T)$ for temperature dependence only

$w_\sigma = (A/E_o).(1/E_\sigma)$ for stress dependence only

$w_{\dot{\sigma}} = (A/E_o).(1/E_{\dot{\sigma}})$ for stress rate dependence only

(ii) Increase in deflection due to one component at a time

$\Delta w_T = (A/E_o).\{(1/E_T)-1\}$ for temperature dependence only

$\Delta w_\sigma = (A/E_o).\{(1/E_\sigma)-1\}$ for stress dependence only

$\Delta w_{\dot{\sigma}} = (A/E_o).\{(1/E_{\dot{\sigma}})-1\}$ for stress rate dependence only

(iii) Cumulative increase in deflection, by adding components in (ii)

$$\Delta w_C = (A/E_o).\{(1/E_T)+(1/E_\sigma)+(1/E_{\dot{\sigma}})-3\}$$

(iv) Combined deflection due to simultaneous dependence of E on all components

$$w = (A/E_o).\{1/[(E_T).(E_\sigma).(E_{\dot{\sigma}})]\}$$

(v) Increase in deflection due to simultaneous dependence of E on all components

$$\Delta w = (A/E_o).\{[1/((E_T).(E_\sigma).(E_{\dot{\sigma}}))]-1\}$$

(vi) The difference between (iii) and (v) is the coupling effect of components affecting the modulus of elasticity. It is equal to

$$(\Delta w - \Delta w_C) = (A/E_o).\{1/[(E_T).(E_\sigma).(E_{\dot{\sigma}})]\}.\{[(2).(E_T).(E_\sigma).(E_{\dot{\sigma}})] - [(E_\sigma).(E_{\dot{\sigma}})]-[(E_T).(E_{\dot{\sigma}})]-[(E_T).(E_\sigma)]+1\}$$

(vii) Symbolically,

$$E = f(T)g(\sigma)h(\dot{\sigma}) = \{f(T)+g(\sigma)+h(\dot{\sigma})\} + \{fg(T,\sigma)+gh(\sigma,\dot{\sigma})+fh(T,\dot{\sigma})+fgh(T,\sigma,\dot{\sigma})\}$$

The quantity within the second set of brackets, { }, represents the coupling effect.

Sample Calculations for the
Beam of HITCAN Demo Problems: From HITCAN outputs

$E_o = 32180$ ksi	$w_o = 0.0135$ inch
$E_T = 0.886$	$w_T = 0.0153$ inch
$E_\sigma = 0.975$	$w_\sigma = 0.0138$
$E_{\dot{\sigma}} = 1.0$	$w_{\dot{\sigma}} = 0.0135$
$E = 27630$ ksi	$w = 0.0157$ inch

(1) Cumulative increase in beam deflection by adding all the components together

(a) Based on deflections output from HITCAN

$\Delta w_C = (w_T - w_o) + (w_\sigma - w_o) + (w_{\dot{\sigma}} - w_o)$

$= (0.0153\text{-}0.0135) + (0.0138\text{-}0.0135) + (0.0135\text{-}0.0135)$

$= 0.0021$ (15.6% of the constant property value)

(b) Based on material properties output from HITCAN

$\Delta w_C = (A/E_o).\{(1/E_T) + (1/E_\sigma) + (1/E_{\dot{\sigma}}) - 3\}$

$= (A/32.18).\{(1/0.886) + (1/0.975) + (1/1.0) - 3\}$

$= (A/32.18).(0.154)$ (15.4% of the constant property value)

Note: This result is for Objective (1).

(2) Increase in deflection due to simultaneous dependence of E on all components

(a) Based on deflections output from HITCAN

$\Delta w = (w - w_o)$

$= (0.0157\text{-}0.0135)$

$= 0.0022$ (16.3% of the constant property value)

(b) Based on material properties output from HITCAN

$\Delta w = (A/E_o).\{[1/((E_T).(E_\sigma).(E_{\dot{\sigma}}))] - 1\}$

$= (A/32.18).\{[1/((0.886).(0.975).(1.0))] - 1\}$

$= (A/32.18).(0.158)$ (15.8% of the constant property value)

Note: This result is for Objective (2).

(3) From (1) and (2) above, the synergistic effect is

(b) Based on material properties output from HITCAN

$\Delta w - \Delta w_C = 0.0022 - 0.0021 = 0.0001$

which is (0.0001/0.0135).(100) = 0.7 % of the constant property

(b) Based on material properties output from HITCAN

$\Delta w - \Delta w_C = (A/32.18).(0.158-0.154) = (A/32.18).(0.004)$

which is (0.004/1.0).(100) = 0.4 % of the constant property

Note: This result is for Objective (3).

Comments: Obviously, the percentages calculated in (1) to (3), (a) & (b) above are different, because the formula, w = (A/E) is not quite correct for the complicated HITCAN demo problem that we ran.

Conclusion: Sample calculations based on properties output from HITCAN demonstrate that, for the case under consideration, the cumulative vs. simultaneous effects of nonlinear property variations on the beam deflection differ by less than 1 %. This effect is due to the coupling of various components of E. The % of the coupling effect, of course, would vary depending on the type of problem under consideration. The coupling effect can be significant for high temperature applications, typical for propulsion structures.

Table I. - HITCAN Capabilities for Composite Materials

Type of Analysis ↓ / Type of Structure →	Beam	Plate	Ring	Curved Panel	Built-up Structure
Static	*tested*	*tested*	*tested*	*tested*	*tested*
Buckling [(a)]	*tested*	*tested*	*tested*	*tested*	*tested*
Load Stepping	*tested*	*tested*	*tested*	*tested*	*tested*
Modal (Natural Vibration Modes) [(b)]	*tested*	*tested*	*tested*	*tested*	*tested*
Time-domain	-	-	-	-	-
Loading					
Mechanical	*tested*	*tested*	*tested*	*tested*	*tested*
Thermal	*tested*	*tested*	*tested*	*tested*	*tested*
Cyclic	-	-	-	-	-
Impact	-	-	-	-	-
Constitutive Models[(c)]					
P = Constant	*tested*	*tested*	*tested*	*tested*	*tested*
$P = f(T)$ (temperature dependence)	*tested*	*tested*	*tested*	*tested*	*tested*
$P = f(\sigma)$ (stress dependence)	*tested*	*tested*	*tested*	*tested*	*tested*
$P = f(\dot{\sigma})$ (stress rate dependence)	*tested*	*tested*	*tested*	*tested*	*tested*
$P = f(t)$ (creep)	-	-	-	-	-
$P = f(T, \sigma, \dot{\sigma})$ (combination)	*tested*	*tested*	*tested*	*tested*	*tested*
$P = f(T, \sigma, \dot{\sigma}, t)$ (creep combination)	-	-	-	-	-
Fiber Degradation	*tested*	*tested*	*tested*	*tested*	*tested*
Fabrication-Induced Stresses	*tested*	*tested*	*tested*	*tested*	*tested*
Ply Orientations [(d)]					
Arbitrary	*tested*	*tested*	*tested*	*tested*	*tested*

(a) Tested 1 buckling mode

(b) Tested 4 vibration modes

(c) Constitutive models: Notation
P: Material properties
T: Temperature
σ : Stress
$\dot{\sigma}$: Stress rate
t : Time

(d) Tested 3 ply orientations:
Unsymmetric: (0/+45/90)
Symmetric: $(0/45)_s$
Balanced: $(0/90)_s$

Table II. - Constituent Material Properties At Unstressed Reference Temperature (70 °F) State

SiC Fiber		Ti-15-3-3-3 Matrix	
P_f	0.11 lb/in^3	P_m	0.172 lb/in^3
E_f	62 Mpsi	E_m	12.3 Mpsi
υ_f	0.3 in/in	υ_m	0.32 in/in
G_f	23.8 Mpsi	G_m	4.7 Mpsi
α_f	1.8 ppm	α_m	4.5 ppm
T_{Mf}	4870 °F	T_{Mm}	1800 °F
S_{f11T}	500 ksi	S_{mT}	130 ksi
S_{f11C}	650 ksi	S_{mC}	130 ksi
S_{f22T}	500 ksi	S_{mS}	91 ksi
S_{f22C}	650 ksi		
S_{f12S}	300 ksi		
D_f	5.6 mils		

Notation:

D: *Fiber Diameter*
E: *Elastic Modulus*
G: *Shear Modulus*
S: *Strength*
T: *Temperature*
P: *Density*
υ: *Poisson's Ratio*
α: *Coefficient of Thermal Expansion*

Subscripts:

c: *Compression*
f: *Fiber*
M: *Melting*
m: *Matrix*
s: *Shear*
T: *Tension*
11: *Direction 11*
22: *Direction 22*
12: *Direction 12*

Table III. - Exponents Used for Multifactor -Interactive Material Behavior Models (Material: Si C/Ti-15-3-3-3)

Material Properties	Variables Affecting Material Properties					
	Temperature		Stress		Stress Rate	
	Matrix	Fiber	Matrix	Fiber	Matrix	Fiber
Modulii	0.5	0.25	0.5	0.25	0.5	0.25
Poisson's Ratios	0.5	0.25	0.5	0.25	0.5	0.25
Strengths	0.5	0.25	0.0	0.0	0.5	0.25
Thermal Expension Coefficients	0.5	0.25	0.0	0.0	0.5	0.25

Table IV. - Summary of Parameters Used
for the Static Analysis (Material[1]:Si C/Ti-15-3-3-3)

Structure[2] → / Parameter ↓	Beam	Plate	Ring	Curved Panel	Built-up Structure
Ply Orientations[3]	$(0/\pm45/90)$	$(0/\pm45/90)$	$(0/\pm45/90)$	$(0/\pm45/90)$	Top $(90/0)_s$ Bottom $(90)_s$ Spars 4 $(0)_6$
Reference Temperature (°F)	70	70	70	70	70
Thermal Load[4] (°F)	1000	1000	1000	1000	1000
Mechanical[5] Load	10 lb [5 a]	200 lb [5 b]	10 lb [5 c]	2000 psi [5 d]	2000 psi [5 e]
Boundary Conditions	Cantilever	Simply Supported	Cantilever	Fixed-Free	Bottom Supported

1: See Tables II and III for material property description.
2: See Figures 5 to 9 for dimensions, etc.
3: First layer is at the top surface and the last one at the bottom surface.
4: Uniform temperature increase in 1 step.
5: Load increase in 1 step.
5 a: Concentrated bending load at the free end center.
5 b: Concentrated bending load at the center point.
5 c: Concentrated bending load at the free end center.
5 d: External pressure at top surface.
5 e: Internal pressure.

Table V. - Summary of Parameters Used for the Buckling Analysis (Material[1]:SiC/Ti-15-3-3-3)

Structure[2] → / Parameter ↓	Beam	Plate	Ring	Curved Panel	Built-up Structure
Ply Orientations[3]	(0/±45/90)	(0/±45/90)	(0/±45/90)	(0/±45/90)	Top: $(90/0)_s$ Bottom: $(90)_s$ Spars: 4 $(0)_s$
Reference Temperature (°F)	70	70	70	70	70
Thermal Load[4] (°F)	1000	1000	1000	1000	1000
Mechanical Load[5]	100 lb[5 a]	25 lb/inch[5 b]	10 lb[5 c]	20 psi[5 d]	10 lb/inch[5 e]
Boundary Conditions	Cantilever	Simply Supported	Cantilever	Fixed-Free	Simply Supported-Free

1: See Tables II and III for material property description.
2: See Figures 10 to 19 for dimensions, etc.
3: First layer is at the top surface and the last one at the bottom surface.
4: Uniform temperature increase in 1 step for the case of combined thermal and mechanical loadings (no temperature for the case of mechanical loading only).
5: Load increase in 1 step.
5 a: Concentrated compressive axial load at the free end center.
5 b: Distributed compressive axial load at 2 shorter edges.
5 c: Concentrated compressive axial load at the free end center.
5 d: External pressure at top surface.
5 e: Distributed compressive axial load at 2 shorter edges.

Table VI. - Summary of Parameters Used for Modal and Load Stepping Analyses (Material[1]:SI C/TI-15-3-3-3)

Structure[2] → / Parameter ↓	Beam	Plate	Ring	Curved Panel	Built-up Structure
Ply Orientations[3]	$(0/\pm45/90)$	$(0/\pm45/90)$	$(0/\pm45/90)$	$(0/\pm45/90)$	Top: $(90/0)_s$ Bottom: $(90)_s$ Spars: 4 $(0)_s$
Reference Temperature (°F)	70	70	70	70	70
Thermal Load[4] (°F)	1000	1000	1000	1000	1000
Mechanical[5] Load	10 lb [5 a]	200 lb [5 b]	10 lb [5 c]	2000 psi[5 d]	2000 psi[5 e]
Boundary Conditions	Cantilever	Simply Supported	Cantilever	Fixed-Free	Bottom Supported

1: See Tables II and III for material property description.
2: See Figures 5 to 9 for dimensions, etc.
3: First layer is at the top surface and the last one at the bottom surface.
4: Uniform temperature increase in 3 step.
5: Load increase in 3 equal steps.
5 a: Concentrated bending load at the free end center.
5 b: Concentrated bending load at the center point.
5 c: Concentrated bending load at the free end center.
5 d: External pressure at top surface.
5 e: Internal pressure.

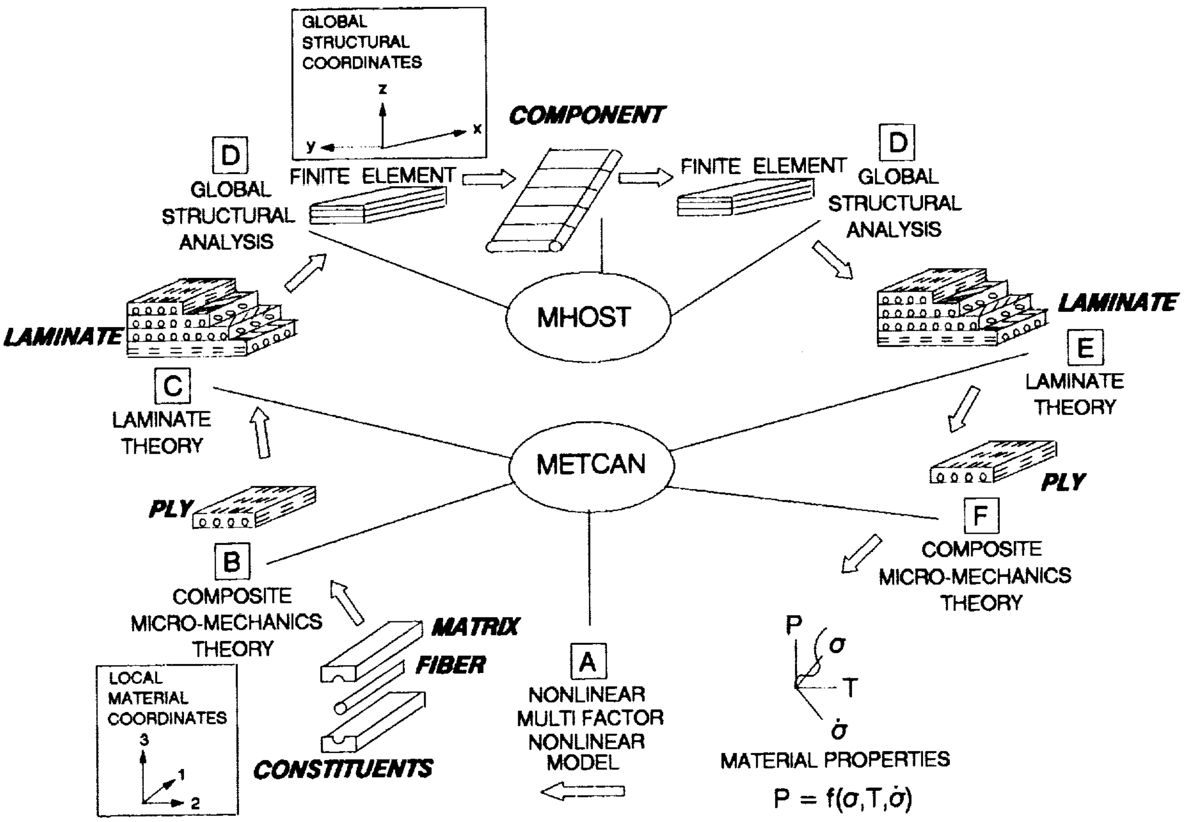

Figure 1 - HITCAN: An Integrated Approach for High Temperature Composite Structural Analysis

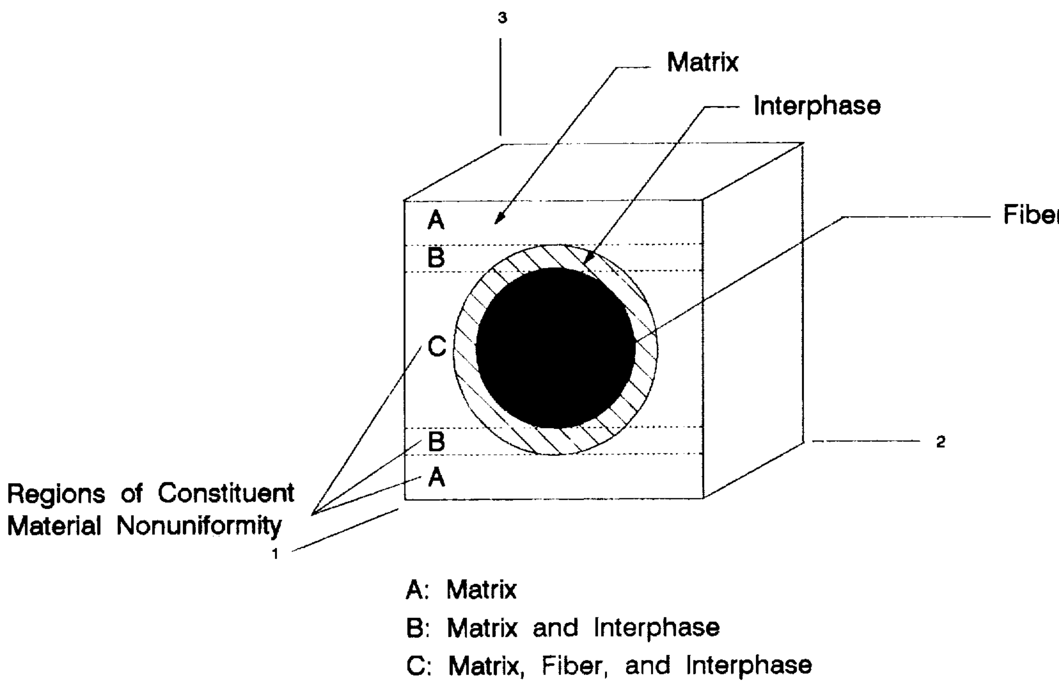

Figure 2 - Schematics for Regions of Constituent Material Nonuniformity

ORIGINAL PAGE IS OF POOR QUALITY

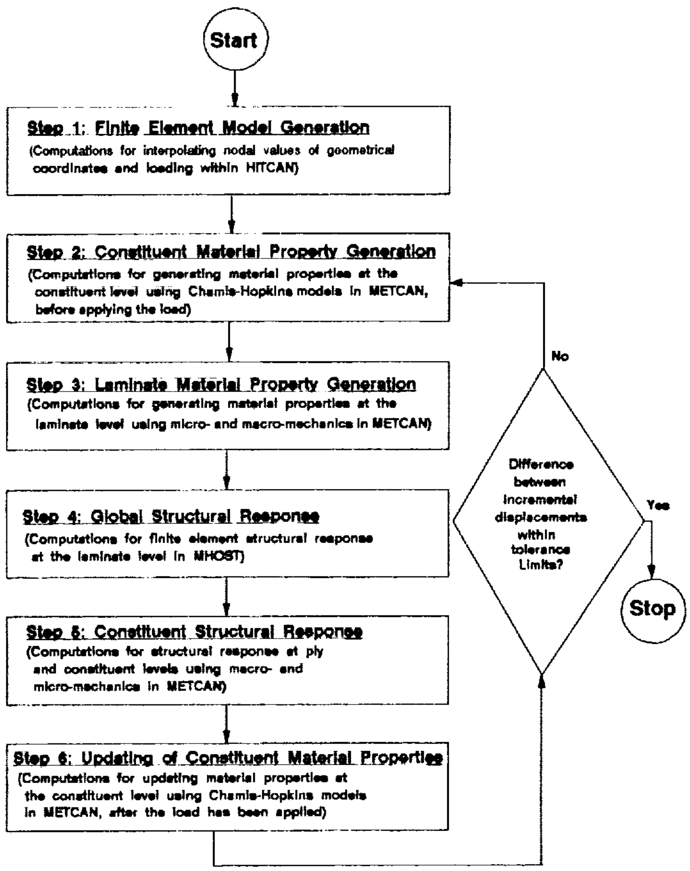

Figure 3 - Flow Chart for HITCAN Computational Procedure

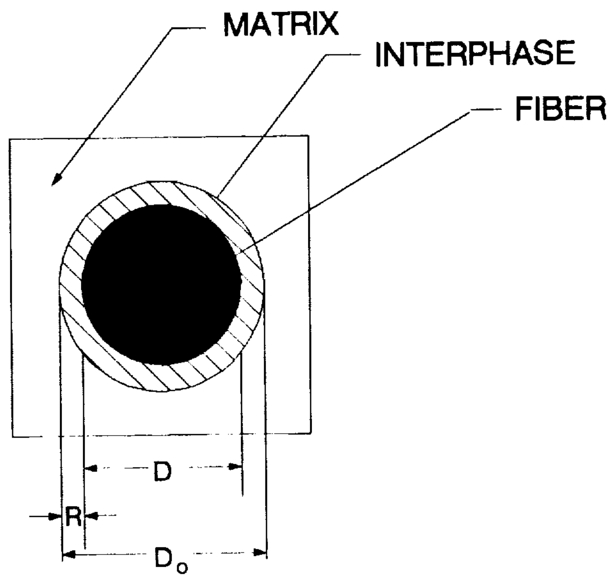

D_o : Original Fiber Diameter

D : Reduced Fiber Diameter

R : Reduction in Fiber Diameter (by an amount specified by the user as a percentage of the original fiber diameter)

Figure 4 - Schematics for Fiber Degradation in Metal Matrix Composites

CANTILEVER BEAM UNDER BENDING AND UNIFORM TEMPERATURE LOADINGS FOR (SI C/TI-15-3-3-3, 0/±45/90); 0.4 FIBER VOLUME RATIO

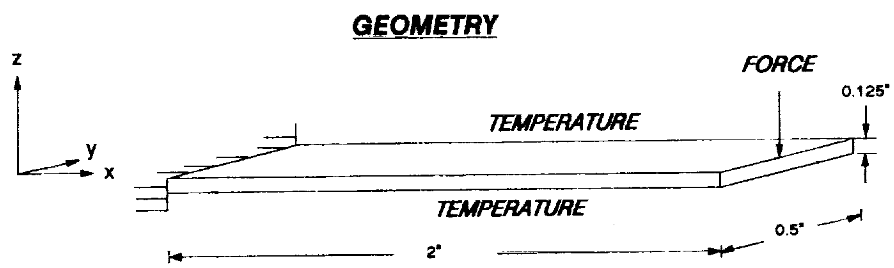

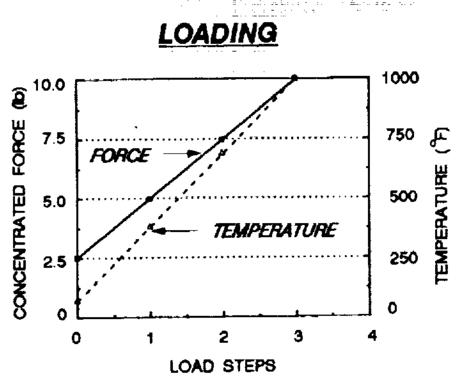

Figure 5 - Geometry and Loading for Beam

SIMPLY SUPPORTED PLATE UNDER BENDING AND UNIFORM TEMPERATURE LOADINGS FOR (SI C/TI-15-3-3-3, 0/±45/90); 0.4 FIBER VOLUME RATIO

GEOMETRY

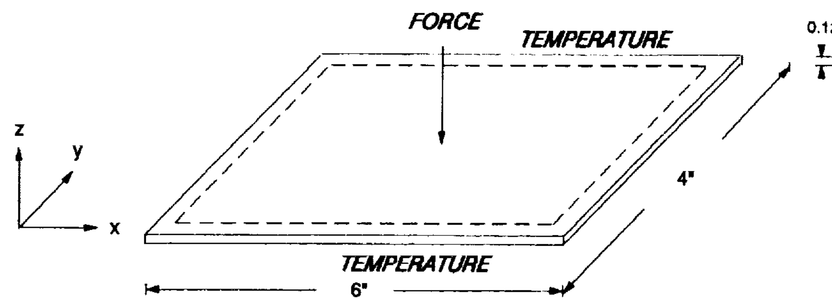

LOADING

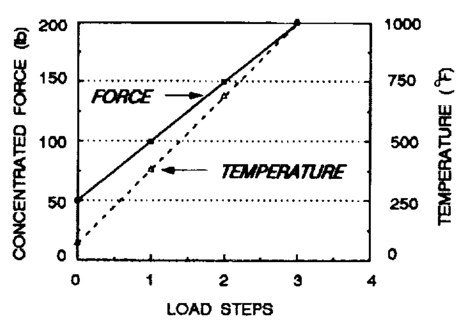

Figure 6 - Geometry and Loading for Plate

CANTILEVER RING UNDER BENDING AND UNIFORM TEMPERATURE LOADINGS FOR (SI C/TI-15-3-3-3, 0/±45/90); 0.4 FIBER VOLUME RATIO

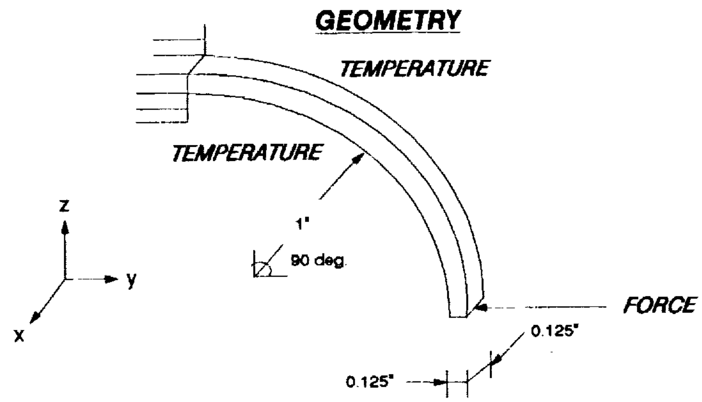

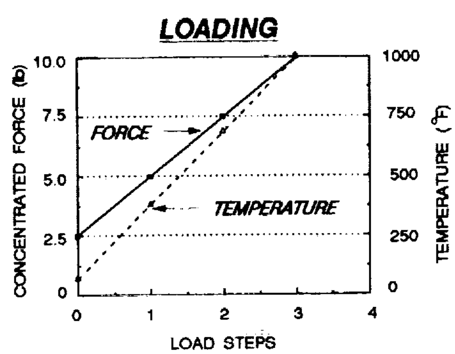

Figure 7 - Geometry and Loading for Ring

FIXED-FREE CURVED PANEL UNDER BENDING AND UNIFORM TEMPERATURE LOADINGS FOR (SI C/TI-15-3-3-3, 0/±45/90); 0.4 FIBER VOLUME RATIO

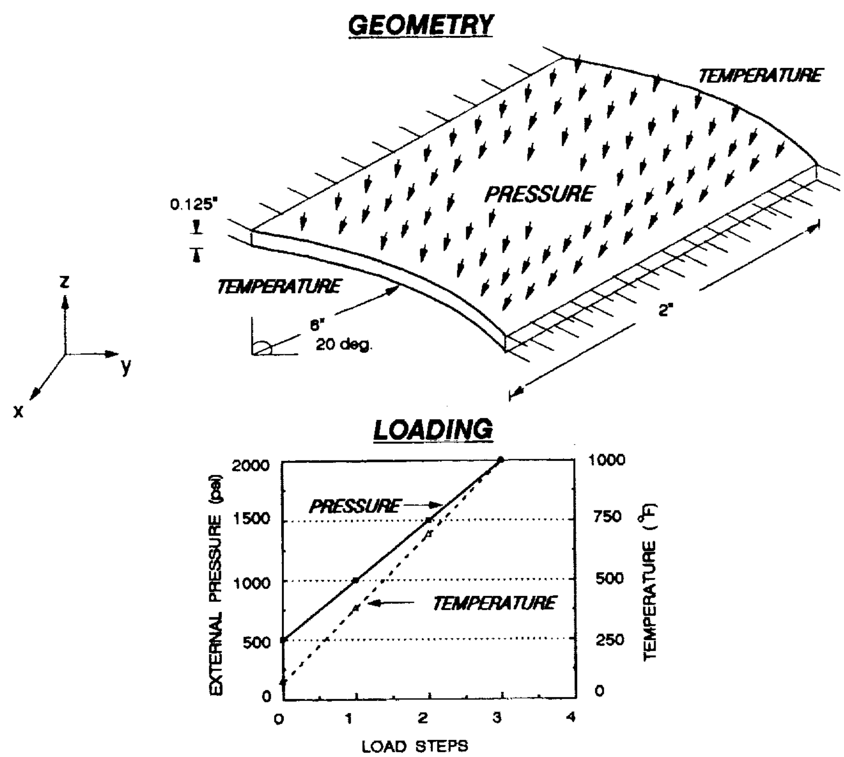

Figure 8 - Geometry and Loading for Curved Panel

BOTTOM SUPPORTED BUILT-UP STRUCTURE UNDER BENDING AND UNIFORM TEMPERATURE LOADINGS FOR (Si C/Ti-15-3-3-3, TOP:$[90,0]_s$, BOTTOM:$[90]_s$, SPARS:$4[0]_s$); 0.4 FIBER VOLUME RATIO

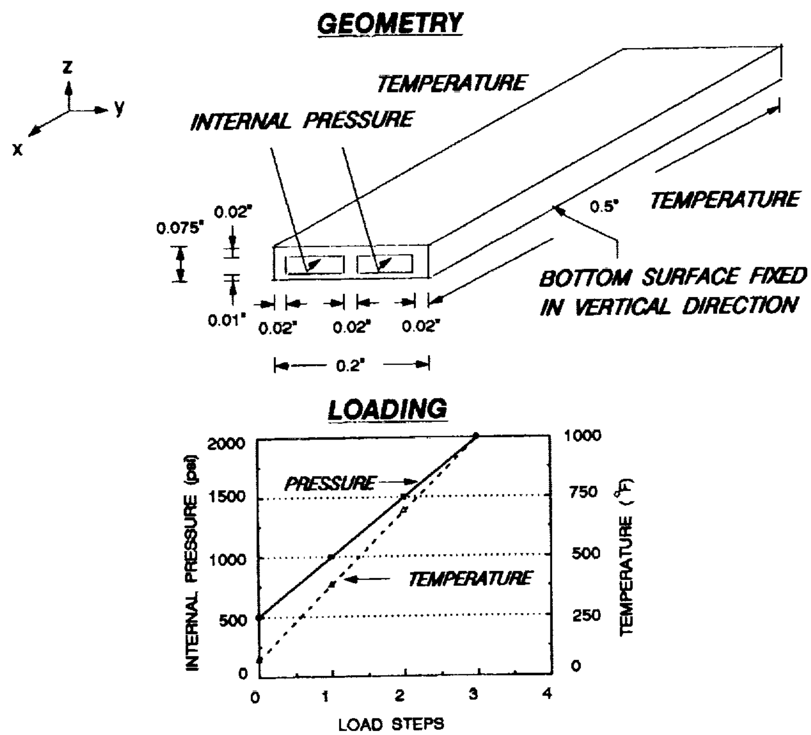

Figure 9 - Geometry and Loading for Built-up Structure

CANTILEVER BEAM UNDER COMPRESSIVE AXIAL AND UNIFORM TEMPERATURE LOADINGS FOR (SI C/TI-15-3-3-3, 0/±45/90); 0.4 FIBER VOLUME RATIO

GEOMETRY AND LOADING

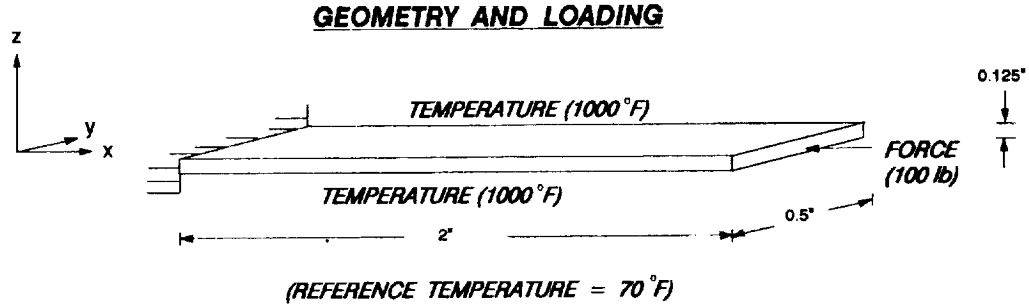

CRITICAL BUCKLING FORCE

(i) UNDER MECHANICAL LOADING ONLY = 1694 lb

(ii) WITH FIBER DEGRADATION, UNDER MECHANICAL LOADING ONLY = 1560 lb

(iii) UNDER THERMO-MECHANICAL LOADING = 1280 lb

Figure 10 - Buckling Analysis for Beam under Thermo-Mechanical Loading

SIMPLY SUPPORTED PLATE UNDER COMPRESSIVE AXIAL AND UNIFORM TEMPERATURE LOADINGS FOR (SI C/TI-15-3-3-3, 0/±45/90); 0.4 FIBER VOLUME RATIO

GEOMETRY AND LOADING

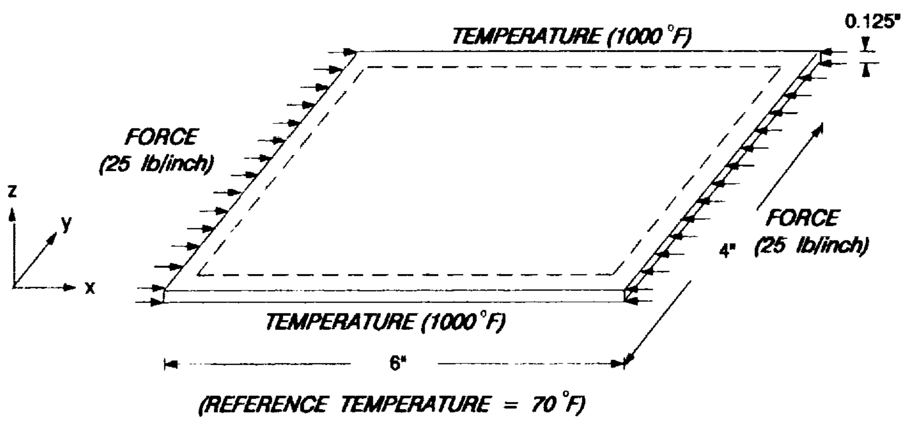

CRITICAL BUCKLING FORCE

(i) UNDER MECHANICAL LOADING ONLY = 939 lb/inch

(ii) WITH FIBER DEGRADATION, UNDER MECHANICAL LOADING ONLY = 901 lb/inch

(iii) UNDER THERMO-MECHANICAL LOADING = 675 lb/inch

Figure 11 - Buckling Analysis for Plate under Thermo-Mechanical Loading

CANTILEVER RING UNDER COMPRESSIVE AXIAL AND UNIFORM TEMPERATURE LOADINGS FOR (SI C/TI-15-3-3-3, 0/±45/90); 0.4 FIBER VOLUME RATIO

GEOMETRY AND LOADING

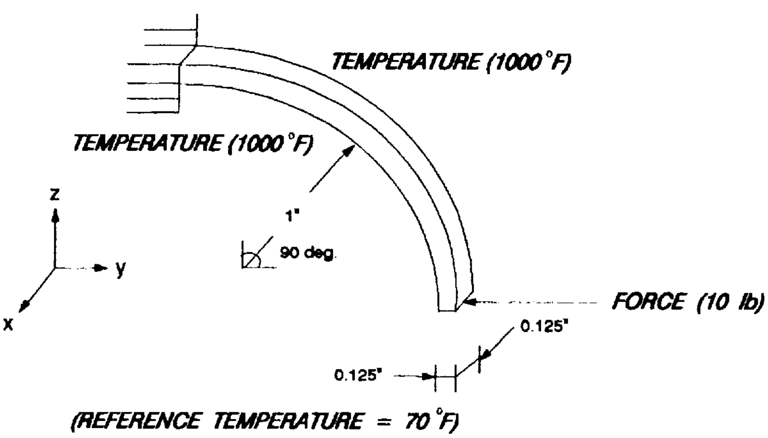

CRITICAL BUCKLING FORCE

(i) UNDER MECHANICAL LOADING ONLY = 1361 lb

(ii) WITH FIBER DEGRADATION, UNDER MECHANICAL LOADING ONLY = 1276 lb

(iii) UNDER THERMO-MECHANICAL LOADING = 1030 lb

Figure 12 - Buckling Analysis for Ring under Thermo-Mechanical Loading

FIXED-FREE CURVED PANEL UNDER EXTERNAL PRESSURE AND UNIFORM TEMPERATURE LOADINGS FOR (Si C/Ti-15-3-3-3, 0/±45/90); 0.4 FIBER VOLUME RATIO

GEOMETRY AND LOADING

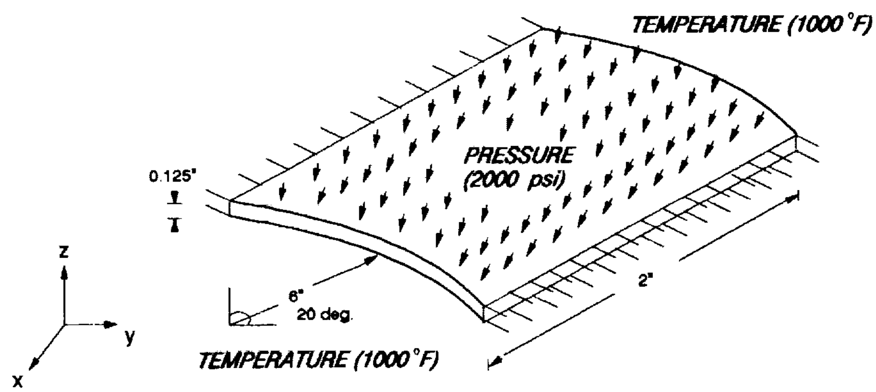

(REFERENCE TEMPERATURE = 70 °F)

CRITICAL BUCKLING PRESSURE

(i) UNDER MECHANICAL LOADING ONLY = 38053 psi

(ii) WITH FIBER DEGRADATION, UNDER MECHANICAL LOADING ONLY = 35437 psi

(iii) UNDER THERMO-MECHANICAL LOADING = 25000 psi

Figure 13 - Buckling Analysis for Curved Panel under Thermo-Mechanical Loading

SIMPLY SUPPORTED-FREE BUILT-UP STRUCTURE UNDER COMPRESSIVE AXIAL AND UNIFORMTEMPERATURE LOADINGS FOR (SI C/TI-15-3-3-3, TOP:$[90,0]_s$, BOTTOM:$[90]_s$, SPARS:$4[0]_s$); 0.4 FIBER VOLUME RATIO

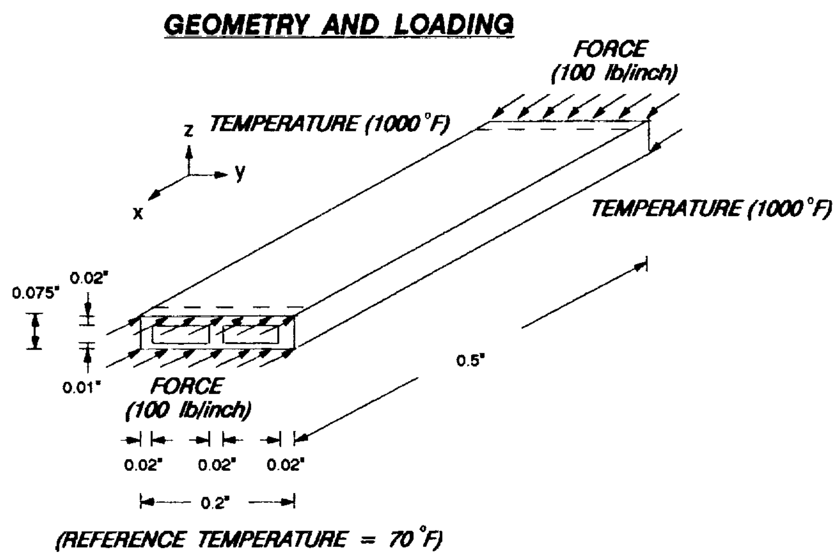

CRITICAL BUCKLING FORCE

(i) UNDER MECHANICAL LOADING ONLY = 2950 lb/inch

(ii) WITH FIBER DEGRADATION, UNDER MECHANICAL LOADING ONLY = 2850 lb/inch

(iii) UNDER THERMO-MECHANICAL LOADING = 2720 lb/inch

Figure 14 - Buckling Analysis for Built-up Structure under Thermo-Mechanical Loading

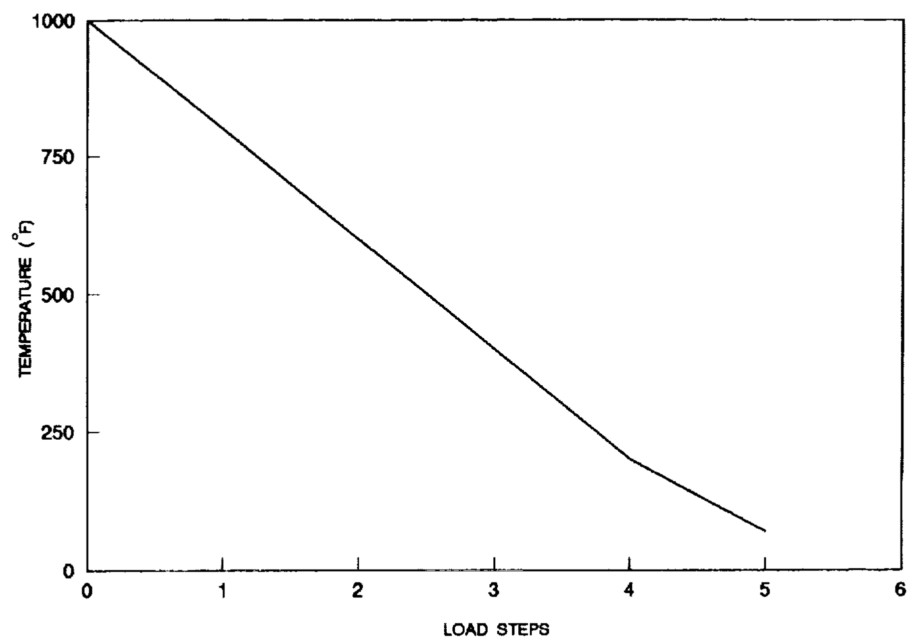

Figure 15 - Fabrication Thermal Cooling Load

CANTILEVER BEAM UNDER BENDING AND UNIFORM TEMPERATURE LOADINGS FOR (Si C/Ti-15-3-3-3, 0/±45/90); 0.4 FIBER VOLUME RATIO

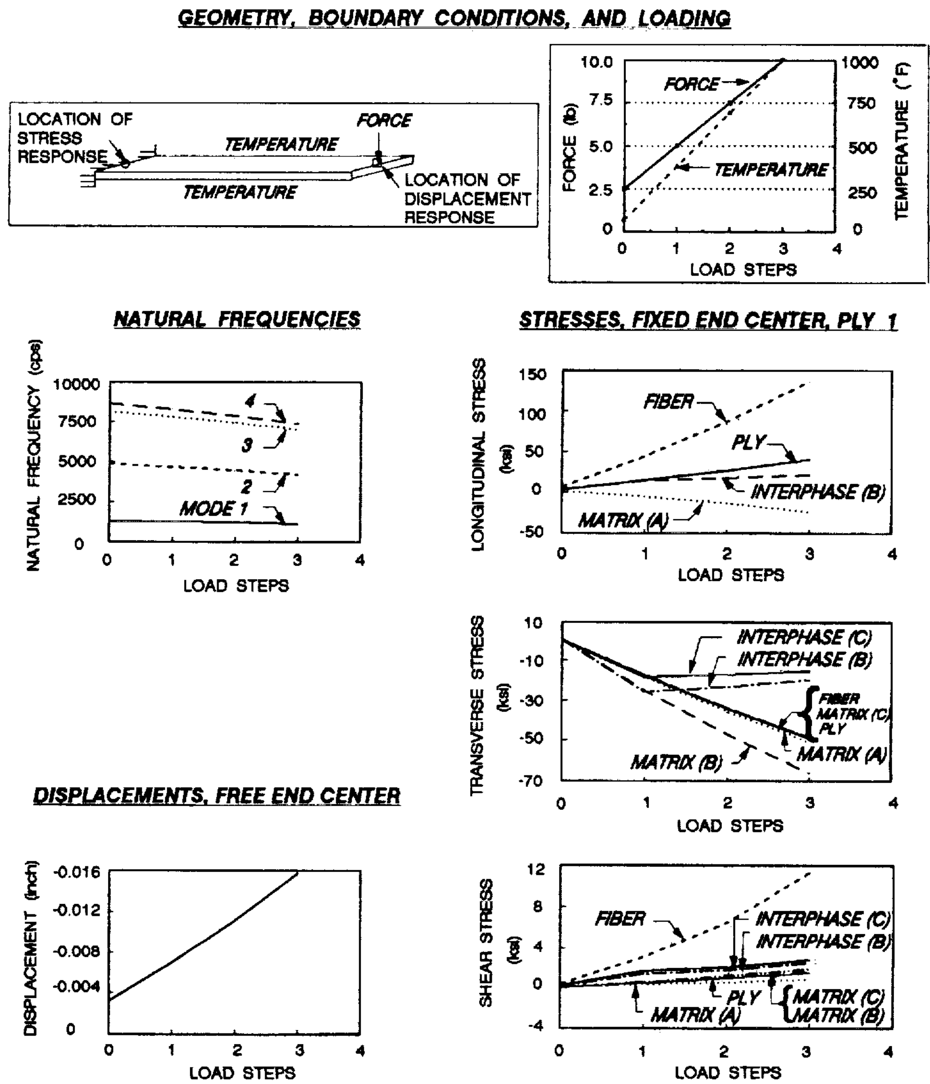

Figure 16 - Base Case Results for Beam

SIMPLY SUPPORTED PLATE UNDER BENDING AND UNIFORM TEMPERATURE LOADINGS FOR (Si C/Ti-15-3-3-3, 0/±45/90); 0.4 FIBER VOLUME RATIO

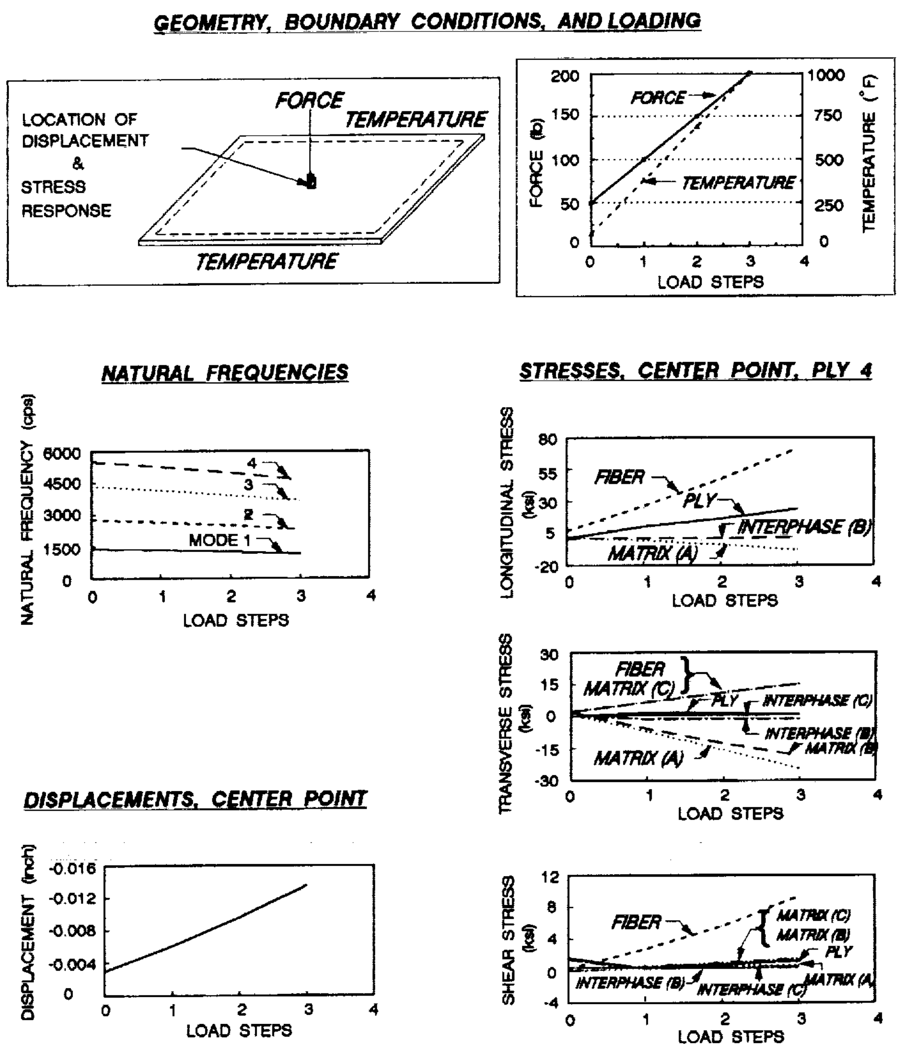

Figure 17 - Base Case Results for Plate

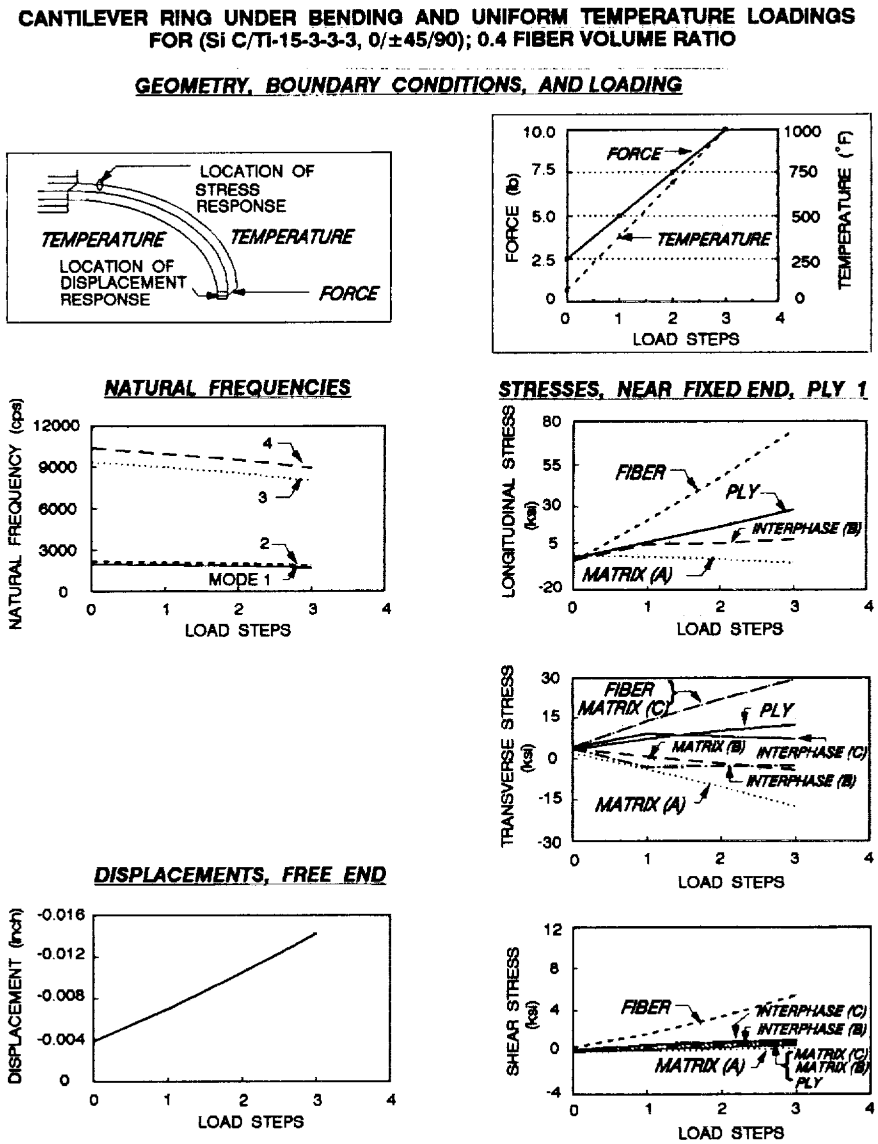

Figure 18 - Base Case Results for Ring

FIXED-FREE CURVED PANEL UNDER BENDING AND UNIFORM TEMPERATURE LOADINGS FOR (SI C/Ti-15-3-3-3, 0/±45/90); 0.4 FIBER VOLUME RATIO

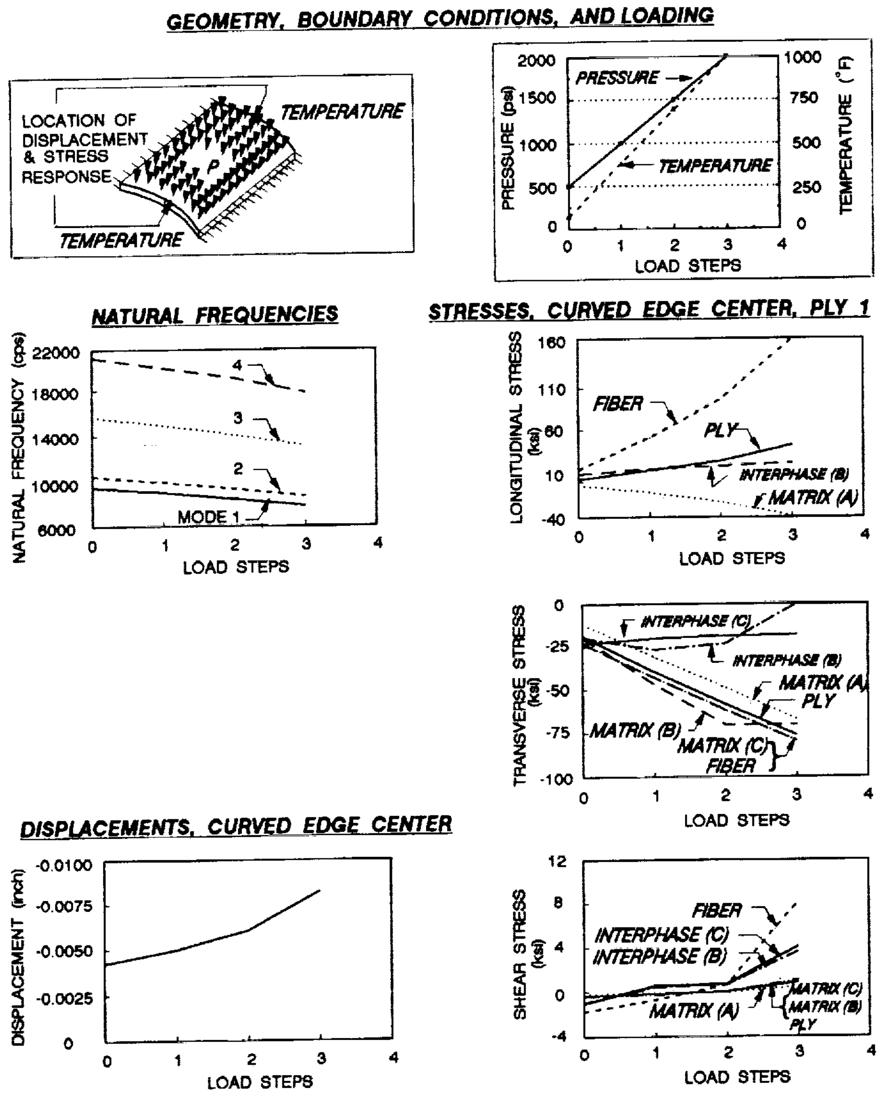

Figure 19 - Base Case Results for Curved Panel

BOTTOM SUPPORTED BUILT-UP STRUCTURE UNDER BENDING AND UNIFORM TEMPERATURE LOADING FOR (Si C/Ti-15-3-3-3, TOP:[90,0]$_s$, BOTTOM:[90]$_s$, SPARS:4[0]$_s$); 0.4 FIBER VOLUME RATIO

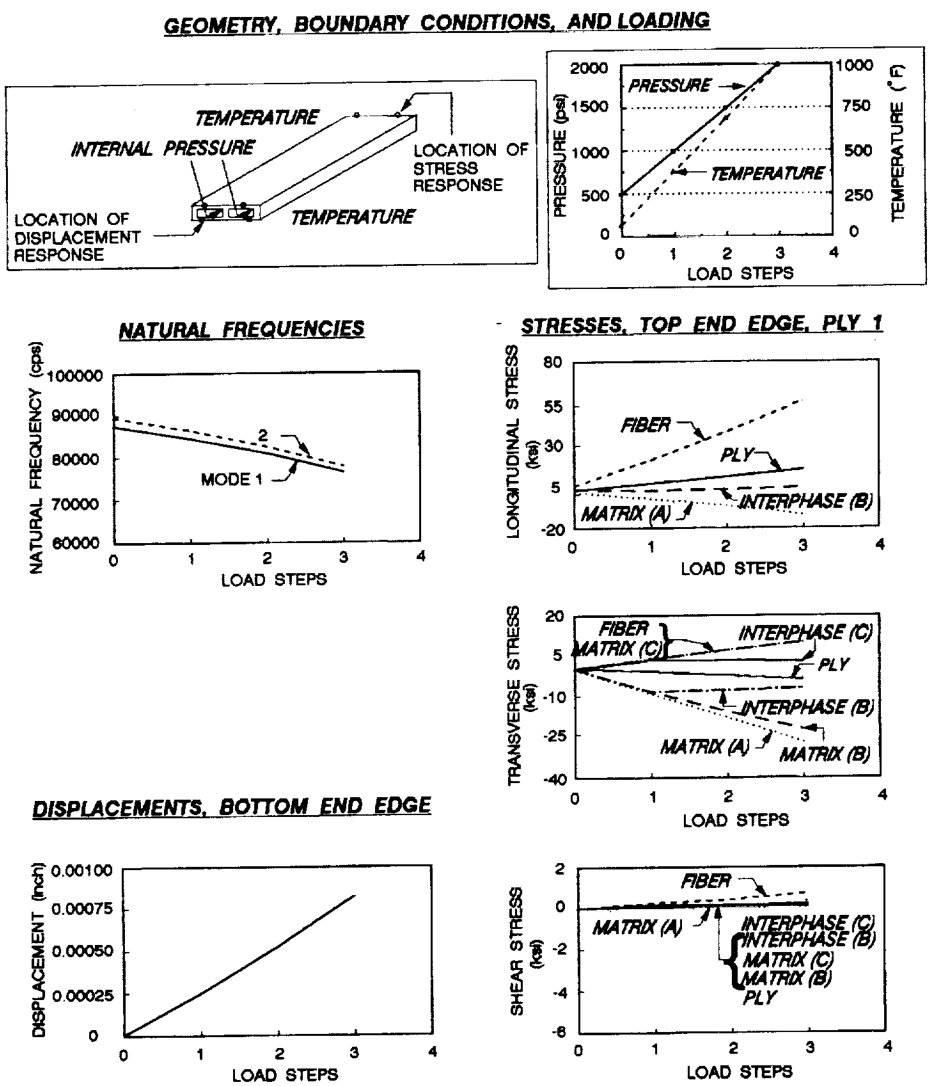

Figure 20 - Base Case Results for Built-up Structure

CANTILEVER BEAM UNDER BENDING AND UNIFORM TEMPERATURE LOADINGS

FOR (SI C/TI-15-3-3-3, 0/±45/90); 0.4 FIBER VOLUME RATIO

RESPONSE: AT LOAD STEP 3

EFFECTS OF

FIBER DEGRADATION

DEGRADATION	DISP. [FREE END CENTER] (inch)	STRESSES, PLY 1 [FIXED END CENTER] (ksi)		
		LONGITUDINAL	TRANSVERSE	SHEAR
NO	-0.0157	40.9	-48.6	1.4
YES	-0.0170	26.3	-36.9	1.1

FABRICATION-INDUCED STRESSES

FABRICATION-INDUCED STRESSES	DISP. [FREE END CENTER] (inch)	STRESSES, PLY 1 [FIXED END CENTER] (ksi)		
		LONGITUDINAL	TRANSVERSE	SHEAR
NO	-0.0157	40.9	-48.6	1.4
YES	-0.0130	30.6	-47.4	0.5

PLY ORIENTATIONS

ORIENTATION	DISP. [FREE END CENTER] (inch)	STRESSES, PLY 1 [FIXED END CENTER] (ksi)		
		LONGITUDINAL	TRANSVERSE	SHEAR
(0/±45/90)	-0.0157	40.9	-48.6	1.4
$(0/45)_S$	-0.0115	20.6	-48.4	0.3
$(0/90)_S$	-0.0115	18.4	-49.0	0.0

CONSTITUTIVE RELATIONSHIPS

(NONLINEAR MULTIFACTOR-INTERACTIVE MODEL)

RELATIONSHIP	DISP. [FREE END CENTER] (inch)	STRESSES, PLY 1 [FIXED END CENTER] (ksi)		
		LONGITUDINAL	TRANSVERSE	SHEAR
P = CONSTANT	-0.0135	36.4	-57.8	1.1
$P = f(T)$ TEMP. DEPENDENCE	-0.0153	44.3	-54.9	1.3
$P = f(\sigma)$ STRESS DEPENDENCE	-0.0138	34.6	-50.2	1.1
$P = f(\dot{\sigma})$ STRESS RATE DEPENDENCE	-0.0135	36.0	-57.8	1.1
$P = f(T, \sigma, \dot{\sigma})$ COMBINATION	-0.0157	40.9	-48.6	1.4

NOTATION:

P = MATERIAL PROPERTY *T = TEMPERATURE*

σ = STRESS *$\dot{\sigma}$ = STRESS RATE*

Figure 21 - Sensitivity Analysis for Beam

SIMPLY SUPPORTED PLATE UNDER BENDING AND UNIFORM TEMPERATURE LOADINGS

FOR (SI C/EI-15-3-3-3, 0/±45/90); 0.4 FIBER VOLUME RATIO

RESPONSE: AT LOAD STEP 3

EFFECTS OF

FIBER DEGRADATION

DEGRADATION	DISP. [CENTER POINT] (inch)	STRESSES, PLY 4 [CENTER POINT] (ksi)		
		LONGITUDINAL	TRANSVERSE	SHEAR
NO	*-0.0135*	*23.9*	*0.8*	*1.3*
YES	*-0.0151*	*21.8*	*1.4*	*1.1*

FABRICATION-INDUCED STRESSES

FABRICATION-INDUCED STRESSES	DISP. [CENTER POINT] (inch)	STRESSES, PLY 4 [CENTER POINT] (ksi)		
		LONGITUDINAL	TRANSVERSE	SHEAR
NO	*-0.0135*	*23.9*	*0.8*	*1.3*
YES	*-0.0140*	*18.4*	*5.8*	*0.4*

PLY ORIENTATIONS

ORIENTATION	DISP. [CENTER POINT] (inch)	STRESSES, PLY 4 [CENTER POINT] (ksi)		
		LONGITUDINAL	TRANSVERSE	SHEAR
(0/±45/90)	*-0.0135*	*23.9*	*0.8*	*1.3*
$(0/45)_S$	*-0.0144*	*11.3*	*7.1*	*-1.6*
$(0/90)_S$	*-0.0149*	*13.5*	*4.7*	*0.0*

CONSTITUTIVE RELATIONSHIPS

(NONLINEAR MULTIFACTOR-INTERACTIVE MODEL)

RELATIONSHIP	DISP. [CENTER POINT] (inch)	STRESSES, PLY 4 [CENTER POINT] (ksi)		
		LONGITUDINAL	TRANSVERSE	SHEAR
P = CONSTANT	*-0.0119*	*22.7*	*2.0*	*1.1*
$P = f(T)$ TEMP. DEPENDENCE	*-0.0133*	*25.5*	*0.9*	*1.3*
$P = f(\sigma)$ STRESS DEPENDENCE	*-0.0121*	*21.5*	*1.9*	*1.1*
$P = f(\dot{\sigma})$ STRESS RATE DEPENDENCE	*-0.0118*	*22.7*	*2.0*	*1.1*
$P = f(T, \sigma, \dot{\sigma})$ COMBINATION	*-0.0135*	*23.9*	*0.8*	*1.3*

NOTATION:

P = MATERIAL PROPERTY ***T = TEMPERATURE***

σ = STRESS ***$\dot{\sigma}$ = STRESS RATE***

Figure 22 - Sensitivity Analysis for Plate

CANTILEVER RING UNDER BENDING AND UNIFORM TEMPERATURE LOADINGS

FOR (SI C/TI-15-3-3-3, 0/±45/90); 0.4 FIBER VOLUME RATIO

RESPONSE: AT LOAD STEP 3

EFFECTS OF

FIBER DEGRADATION

DEGRADATION	DISP. [FREE END] (inch)	STRESSES, PLY 1 [NEAR FIXED END] (ksi)		
		LONGITUDINAL	TRANSVERSE	SHEAR
NO	-0.0142	27.4	12.6	0.7
YES	-0.0154	25.5	14.8	0.6

FABRICATION-INDUCED STRESSES

FABRICATION-INDUCED STRESSES	DISP. [FREE END] (inch)	STRESSES, PLY 1 [NEAR FIXED END] (ksi)		
		LONGITUDINAL	TRANSVERSE	SHEAR
NO	-0.0142	27.4	12.6	0.7
YES	-0.0128	18.4	15.3	-0.3

PLY ORIENTATIONS

ORIENTATION	DISP. [FREE END] (inch)	STRESSES, PLY 1 [NEAR FIXED END] (ksi)		
		LONGITUDINAL	TRANSVERSE	SHEAR
(0/±45/90)	-0.0142	27.4	12.6	0.7
$(0/45)_S$	-0.0193	21.5	24.6	-1.9
$(0/90)_S$	-0.0177	26.1	19.9	-0.4

CONSTITUTIVE RELATIONSHIPS

(NONLINEAR MULTIFACTOR-INTERACTIVE MODEL)

RELATIONSHIP	DISP. [FREE END] (inch)	STRESSES, PLY 1 [NEAR FIXED END] (ksi)		
		LONGITUDINAL	TRANSVERSE	SHEAR
$P = \text{CONSTANT}$	-0.0124	26.3	17.5	0.6
$P = f(T)$ TEMP. DEPENDENCE	-0.0139	35.3	10.5	1.5
$P = f(\sigma)$ STRESS DEPENDENCE	-0.0127	24.1	15.7	0.5
$P = f(\dot{\sigma})$ STRESS RATE DEPENDENCE	-0.0124	26.3	17.5	0.6
$P = f(T, \sigma, \dot{\sigma})$ COMBINATION	-0.0142	27.4	12.6	0.7

NOTATION:

P = MATERIAL PROPERTY — *T = TEMPERATURE*

σ = STRESS — *$\dot{\sigma}$ = STRESS RATE*

Figure 23 - Sensitivity Analysis for Ring

FIXED-FREE CURVED PANEL UNDER BENDING AND UNIFORM TEMPERATURE LOADINGS

FOR (SI C/TI-15-3-3-3, 0/±45/90); 0.4 FIBER VOLUME RATIO

RESPONSE: AT LOAD STEP 3

EFFECTS OF

FIBER DEGRADATION

DEGRADATION	DISP. [CURVED EDGE CENTER] (inch)	STRESSES, PLY 1 [CURVED EDGE CENTER] (ksi) LONGITUDINAL	TRANSVERSE	SHEAR
NO	*-0.00827*	*40.7*	*-75.9*	*1.7*
YES	*-0.00799*	*34.7*	*-75.1*	*1.7*

FABRICATION-INDUCED STRESSES

FABRICATION-INDUCED STRESSES	DISP. [CURVED EDGE CENTER] (inch)	STRESSES, PLY 1 [CURVED EDGE CENTER] (ksi) LONGITUDINAL	TRANSVERSE	SHEAR
NO	*-0.00827*	*40.7*	*-75.9*	*1.7*
YES	*-0.00873*	*25.9*	*-72.3*	*-0.6*

PLY ORIENTATIONS

ORIENTATION	DISP. [CURVED EDGE CENTER] (inch)	STRESSES, PLY 1 [CURVED EDGE CENTER] (ksi) LONGITUDINAL	TRANSVERSE	SHEAR
(0/±45/90)	*-0.00827*	*40.7*	*-75.9*	*1.7*
$(0/45)_s$	*-0.01060*	*10.9*	*-67.7*	*0.2*
$(0/90)_s$	*-0.00499*	*8.3*	*-64.3*	*0.0*

CONSTITUTIVE RELATIONSHIPS

(NONLINEAR MULTIFACTOR-INTERACTIVE MODEL)

RELATIONSHIP	DISP. [CURVED EDGE CENTER] (inch)	STRESSES, PLY 1 [CURVED EDGE CENTER] (ksi) LONGITUDINAL	TRANSVERSE	SHEAR
P = CONSTANT	*-0.00578*	*28.4*	*-85.8*	*0.2*
$P = f(T)$ TEMP. DEPENDENCE	*-0.00686*	*44.9*	*-74.1*	*1.0*
$P = f(\sigma)$ STRESS DEPENDENCE	*-0.00688*	*29.0*	*-76.7*	*0.2*
$P = f(\dot{\sigma})$ STRESS RATE DEPENDENCE	*-0.00577*	*28.4*	*-85.8*	*0.2*
$P = f(T, \sigma, \dot{\sigma})$ COMBINATION	*-0.00827*	*40.7*	*-75.9*	*1.7*

NOTATION:

P = MATERIAL PROPERTY *T = TEMPERATURE*

σ = STRESS *$\dot{\sigma}$ = STRESS RATE*

Figure 24 - Sensitivity Analysis for Curved Panel

BOTTOM SUPPORTED BUILT-UP STRUCTURE UNDER BENDING AND UNIFORM TEMPERATURE LOADINGS FOR (SI C/TI-15-3-3-3, TOP:$[90,0]_s$, BOTTOM:$[90]_s$, SPARS:$4[0]_s$); 0.4 FIBER VOLUME RATIO

RESPONSE: AT LOAD STEP 3

EFFECTS OF

FIBER DEGRADATION

DEGRADATION	DISP. [BOTTOM END EDGE] (Inch)	STRESSES, PLY 1 [TOP END EDGE] (ksi)		
		LONGITUDINAL	TRANSVERSE	SHEAR
NO	*0.000823*	*15.2*	*-3.3*	*0.1*
YES	*0.000886*	*14.4*	*-2.6*	*0.1*

FABRICATION-INDUCED STRESSES

FABRICATION-INDUCED STRESSES	DISP. [BOTTOM END EDGE] (Inch)	STRESSES, PLY 1 [TOP END EDGE] (ksi)		
		LONGITUDINAL	TRANSVERSE	SHEAR
NO	*0.000823*	*15.2*	*-3.3*	*0.1*
YES	*0.000420*	*12.2*	*0.5*	*0.02*

CONSTITUTIVE RELATIONSHIPS

(NONLINEAR MULTIFACTOR-INTERACTIVE MODEL)

RELATIONSHIP	DISP. [BOTTOM END EDGE] (inch)	STRESSES, PLY 1 [TOP END EDGE] (ksi)		
		LONGITUDINAL	TRANSVERSE	SHEAR
P = CONSTANT	*0.000710*	*15.2*	*-2.6*	*0.1*
P = f(T) TEMP. DEPENDENCE	*0.000828*	*16.4*	*-3.6*	*1.0*
P = f(σ) STRESS DEPENDENCE	*0.000707*	*14.3*	*-2.4*	*0.1*
P = f($\dot{\sigma}$) STRESS RATE DEPENDENCE	*0.000710*	*15.2*	*-2.6*	*0.1*
P = f(T, σ, $\dot{\sigma}$) COMBINATION	*0.000823*	*15.2*	*-3.3*	*0.1*

NOTATION:
P = MATERIAL PROPERTY *T = TEMPERATURE*
σ = STRESS *$\dot{\sigma}$ = STRESS RATE*

Figure 25 - Sensitivity Analysis for Built-up Structure

ORIGINAL PAGE IS
OF POOR QUALITY

CANTILEVER BEAM UNDER BENDING AND UNIFORM TEMPERATURE LOADINGS FOR (SI C/TI-15-3-3-3, 0/±45/90); 0.4 FIBER VOLUME RATIO

EFFECT OF MATERIAL PROPERTY VARIATIONS ON DISPLACEMENT AT FREE END CENTER

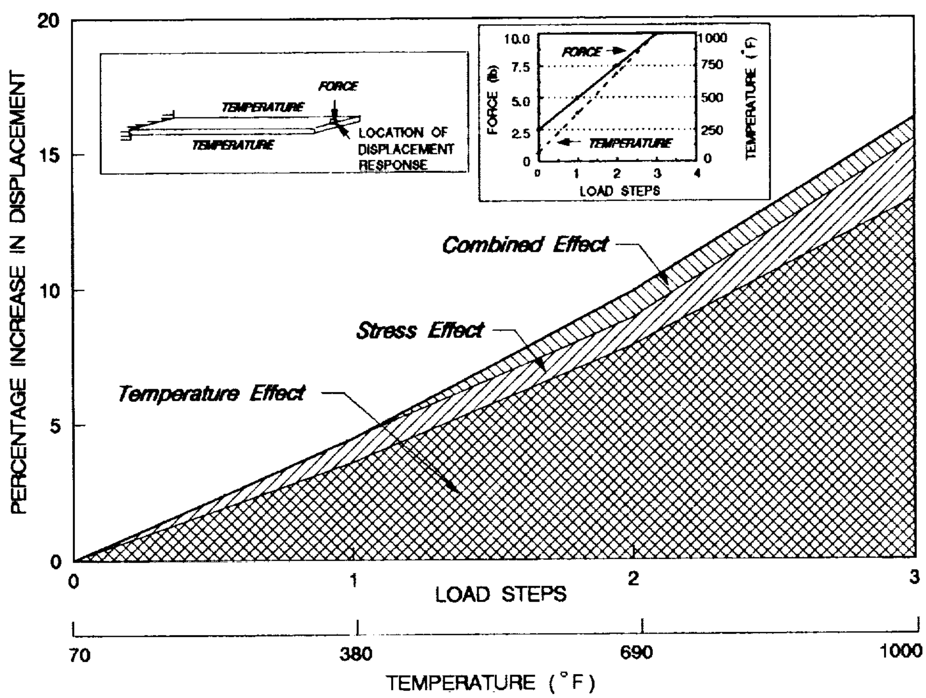

Figure 26 - Sensitivity to Constitutive Models for Beam

SIMPLY SUPPORTED PLATE UNDER BENDING AND UNIFORM TEMPERATURE LOADINGS FOR (SI C/TI-15-3-3-3, 0/±45/90); 0.4 FIBER VOLUME RATIO

EFFECT OF MATERIAL PROPERTY VARIATIONS ON DISPLACEMENT AT CENTER POINT

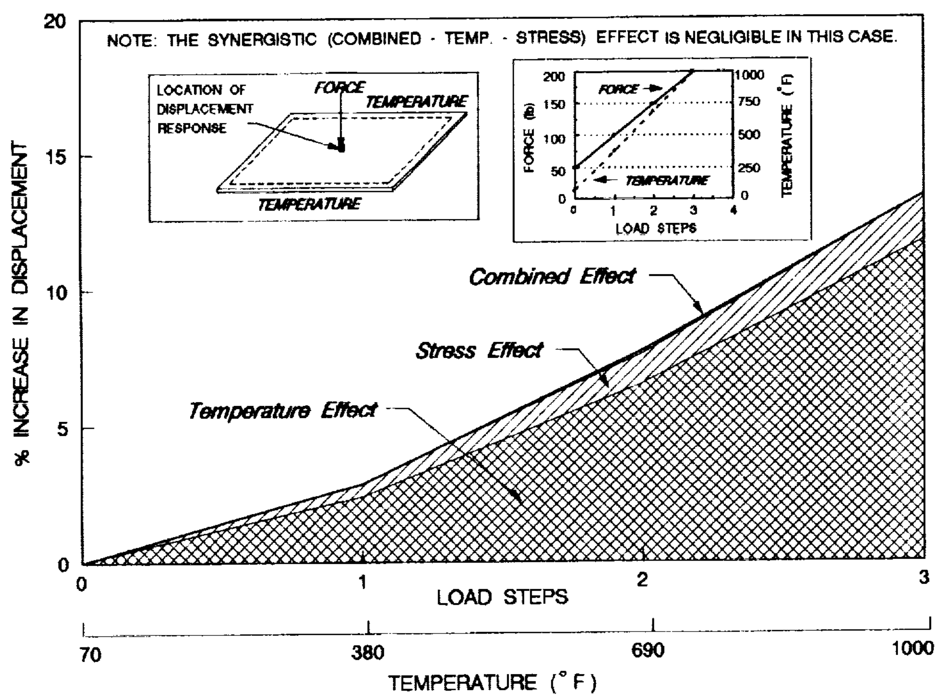

Figure 27 - Sensitivity to Constitutive Models for Plate

CANTILEVER RING UNDER BENDING AND UNIFORM TEMPERATURE LOADINGS FOR (SI C/TI-15-3-3-3, 0±45/90); 0.4 FIBER VOLUME RATIO

EFFECT OF MATERIAL PROPERTY VARIATIONS ON DISPLACEMENT AT FREE END

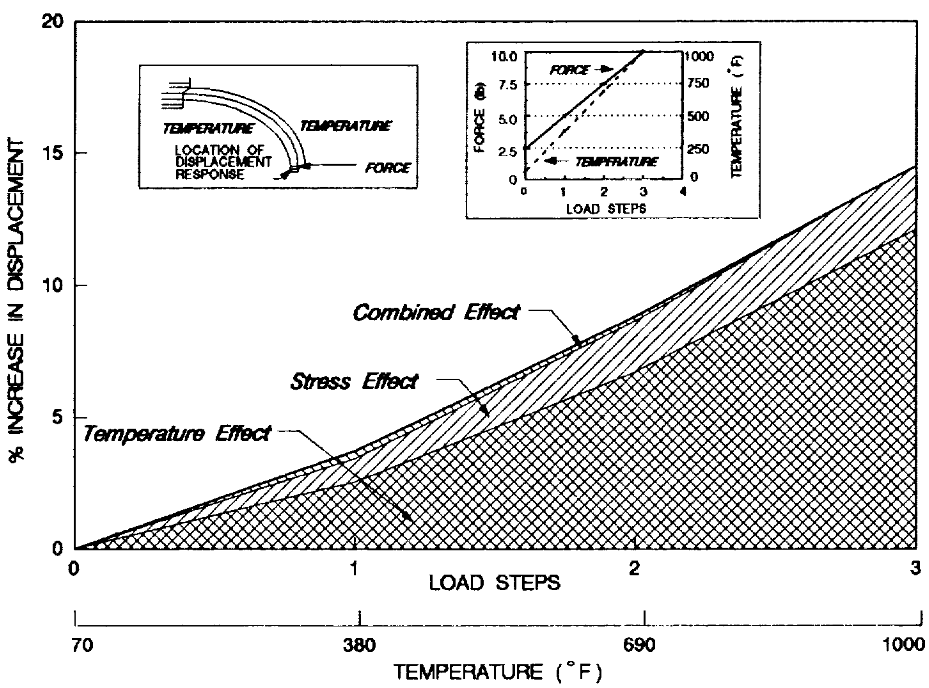

Figure 28 - Sensitivity to Constitutive Models for Ring

FIXED-FREE CURVED PANEL UNDER BENDING AND UNIFORM TEMPERATURE LOADINGS FOR (SI C/TI-15-3-3-3, 0/±45/90); 0.4 FIBER VOLUME RATIO

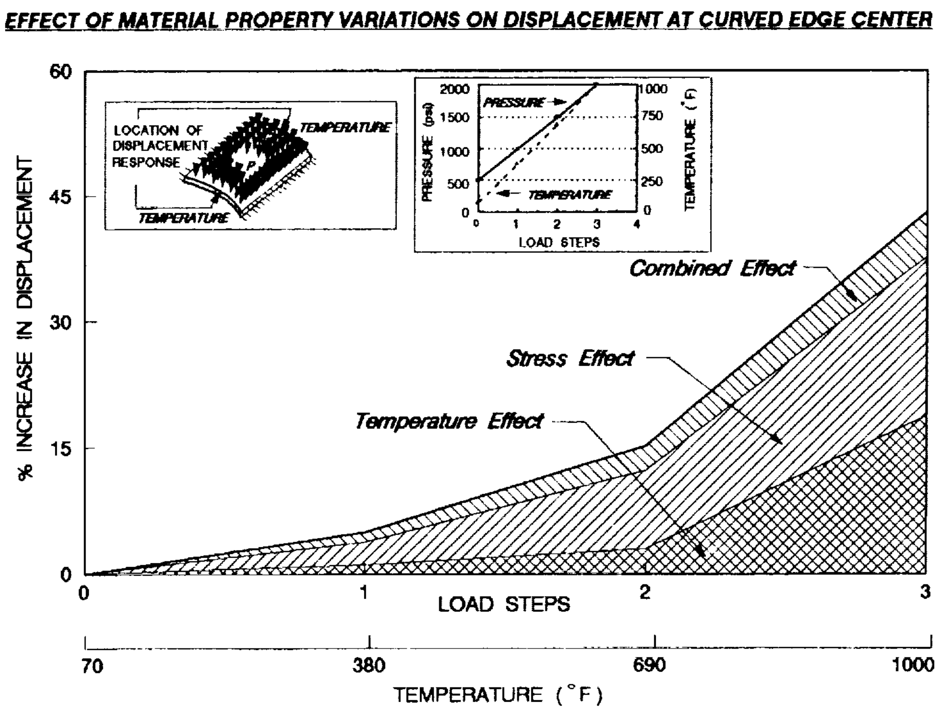

Figure 29 - Sensitivity to Constitutive Models for Curved Panel

BOTTOM SUPPORTED BUILT-UP STRUCTURE UNDER BENDING AND UNIFORM TEMPERATURE LOADINGS FOR (SI C/TI-15-3-3-3, TOP:[90,0]$_s$, BOTTOM:[90]$_s$, SPARS:4[0]$_s$); 0.4 FIBER VOLUME RATIO

EFFECT OF MATERIAL PROPERTY VARIATIONS ON DISPLACEMENT AT BOTTOM END EDGE

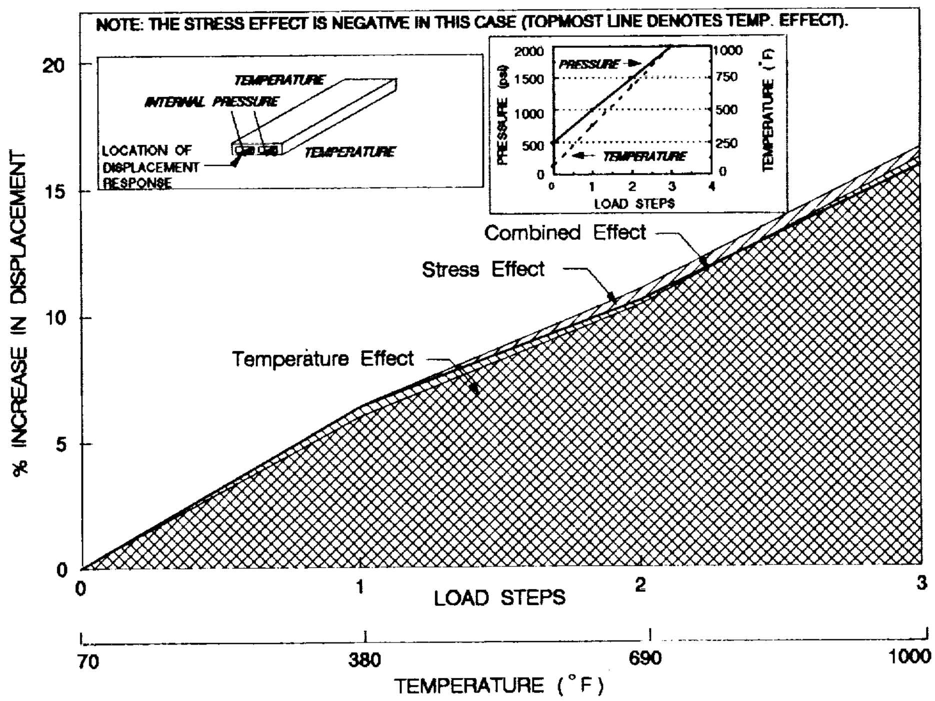

Figure 30 - Sensitivity to Constitutive Models for Built-up Structure

NASA
National Aeronautics and Space Administration

Report Documentation Page

1. Report No. NASA TM-102560	2. Government Accession No.	3. Recipient's Catalog No.
4. Title and Subtitle Demonstration of Capabilities of High Temperature Composites Analyzer Code HITCAN		5. Report Date March 1990
		6. Performing Organization Code
7. Author(s) Surendra N. Singhal, Joseph J. Lackney, Christos C. Chamis, and Pappu L.N. Murthy		8. Performing Organization Report No. E-5380
		10. Work Unit No. 763-01-4B
9. Performing Organization Name and Address National Aeronautics and Space Administration Lewis Research Center Cleveland, Ohio 44135-3191		11. Contract or Grant No.
		13. Type of Report and Period Covered Technical Memorandum
12. Sponsoring Agency Name and Address National Aeronautics and Space Administration Washington, D.C. 20546-0001		14. Sponsoring Agency Code

15. Supplementary Notes

Surendra N. Singhal and Joseph J. Lackney, Sverdrup Technology, Inc., NASA Lewis Research Center Group, Cleveland, Ohio 44135. Christos C. Chamis and Pappu L.N. Murthy, NASA Lewis Research Center.

16. Abstract

The present report demonstrates the capabilities of a high temperature composites analyzer code, HITCAN which predicts global structural and local stress-strain response of multilayered metal matrix composite structures. The response can be determined both at the constituent (fiber, matrix, and interphase) and the structure level and including the fabrication process effects. The thermo-mechanical properties of the constituents are considered to be nonlinearly dependent on several parameters including temperature, stress, and stress rate. The computational procedure employs an incremental iterative nonlinear approach utilizing a multifactor-interactive constituent material behavior model. Various features of the code are demonstrated through example problems for typical structures.

17. Key Words (Suggested by Author(s))	18. Distribution Statement
Buckling; Composite mechanics; Computer codes; Fabrication stresses; Fiber composites; Metal matrix; Finite element analysis; Global response; High temperature composites; Interphase; Interphase degradation; Laminate analysis; Load stepping; Local response; Material nonlinearities; Mechanical properties; Micro stresses; Micromechanics; Modal analysis; Nonlinear behavior; Stress analysis; Structural analysis; Thermal properties; Thermo mechanical analysis; Vibration frequencies	Unclassified – Unlimited Subject Category 39

19. Security Classif. (of this report)	20. Security Classif. (of this page)	21. No. of pages	22. Price*
Unclassified	Unclassified	54	A04

*For sale by the National Technical Information Service, Springfield, Virginia 22161